Title

The Carboxy-Terminal Tails of Septins Cdc11 and Shs1 Recruit Myosin-II Binding Factor Bni5 to the Bud Neck in Saccharomyces cerevisiae

Journal

Genetics, 200(3)

ISSN

0016-6731

Authors

Finnigan, Gregory C
Booth, Elizabeth A
Duvalyan, Angela
et al.

Publication Date

2015-07-01

DOI

10.1534/genetics.115.176503

Peer reviewed

The Carboxy-Terminal Tails of Septins Cdc11 and Shs1 Recruit Myosin-II Binding Factor Bni5 to the Bud Neck in *Saccharomyces cerevisiae*

Gregory C. Finnigan, Elizabeth A. Booth, Angela Duvalyan, Elizabeth N. Liao, and Jeremy Thorner[1]
Division of Biochemistry, Biophysics and Structural Biology, Department of Molecular and Cell Biology, University of California, Berkeley, California 94720-3202

ABSTRACT Septins are a conserved family of GTP-binding proteins that form heterooctameric complexes that assemble into higher-order structures. In yeast, septin superstructure at the bud neck serves as a barrier to separate a daughter cell from its mother and as a scaffold to recruit the proteins that execute cytokinesis. However, how septins recruit specific factors has not been well characterized. In the accompanying article in this issue, (Finnigan *et al.* 2015), we demonstrated that the C-terminal extensions (CTEs) of the alternative terminal subunits of septin heterooctamers, Cdc11 and Shs1, share a role required for optimal septin function *in vivo*. Here we describe our use of unbiased genetic approaches (both selection of dosage suppressors and analysis of synthetic interactions) that pinpointed Bni5 as a protein that interacts with the CTEs of Cdc11 and Shs1. Furthermore, we used three independent methods—construction of chimeric proteins, noncovalent tethering mediated by a GFP-targeted nanobody, and imaging by fluorescence microscopy—to confirm that a physiologically important function of the CTEs of Cdc11 and Shs1 is optimizing recruitment of Bni5 and thereby ensuring efficient localization at the bud neck of Myo1, the type II myosin of the actomyosin contractile ring.

Related article in *GENETICS*: Finnigan, G. C. *et al.*, 2015 Comprehensive Genetic Analysis of Paralogous Terminal Septin Subunits Shs1 and Cdc11 in *Saccharomyces cerevisiae*. Genetics **200:** 821–841.

KEYWORDS yeast; cytokinesis; complexes; filaments; mutants

SEPTIN-based structures in metazoans are frequently found at the boundaries between cellular compartments (Saarikangas and Barral 2011; Trimble and Grinstein 2015). The tissue specificity with which septin genes are expressed, and/or their mRNAs undergo alternative splicing, is consistent with specific septins and septin isoforms playing distinct roles in particular developmental and physiological processes (Roeseler *et al.* 2009; Hall and Russell 2012; Dolat *et al.* 2014). A prominent septin-containing structure is located at the bottom of the neck of each small membranous protrusion (dendritic spine) that projects from the dendrites that extend from the cell body of a neuron (Tada *et al.* 2007; Ewers *et al.* 2014), indicating some role in neurogenesis. A discrete septin-containing structure, dubbed the annulus, separates the head and midpiece from the flagellum in mature mammalian sperm and is required for sperm motility (Sugino *et al.* 2008; Toure *et al.* 2011). Similarly, septin function has been implicated in the amoeboid motility of T cells by promoting membrane retraction (Tooley *et al.* 2009; Gilden *et al.* 2012). Septin-containing structures are found at the base of the primary (nonmotile) cilium and at discrete regions along the axoneme, suggesting roles in ciliogenesis and in the signaling functions of this sensory organelle (Hu *et al.* 2010; Ghossoub *et al.* 2013; Sharma *et al.* 2013). Septin "cages" assemble around intracellular bacterial pathogens or the vacuolar inclusions that contain them, but whether caging serves as a first line of defense against their spread (Mostowy *et al.* 2010), or is exploited by the microbes to promote their spread (Volceanov *et al.* 2014), has not been resolved. In all the instances described above, just what other cellular factors are recruited via direct physical association with any specific septin and whether that interaction is required for the

doi: 10.1534/genetics.115.176503
Manuscript received March 17, 2015; accepted for publication May 8, 2015; published Early Online May 12, 2015.
Supporting information is available online at www.genetics.org/lookup/suppl/doi:10.1534/genetics.115.176503/-/DC1.
[1]Corresponding author: Department of Molecular and Cell Biology, University of California, Room 16, Barker Hall, Berkeley, CA 94720-3202.
E-mail: jthorner@berkeley.edu

biological function of the septin-based structure at its observed location has not been delineated.

In budding yeast *Saccharomyces cerevisiae*, a prominent collar composed of septin filaments is assembled in a cell cycle-specific manner at the neck between a mother cell and its daughter and is required for the execution of cytokinesis and septation (Roncero and Sánchez 2010; Wloka and Bi 2012). Likewise, during each round of cell division of a mammalian cell, a septin-based ring-like structure is found at the site of cytokinesis and, of the 13 mammalian septin gene products, SEPT9 appears to be especially critical for the role that septins play in the abscission needed to separate two daughter cells (Estey *et al.* 2010; Füchtbauer *et al.* 2011). SEPT9 (and its closest paralogs, SEPT3 and SEPT12) are alternative subunits that can occupy the end position in mammalian septin heterooctamers (Kim *et al.* 2011; Sellin *et al.* 2011; Sellin *et al.* 2014) just as do the alternative terminal subunits Cdc11 and Shs1 in *S. cerevisiae* heterooctamers (Bertin *et al.* 2008; Garcia *et al.* 2011; McMurray *et al.* 2011; Finnigan *et al.* 2015).

As documented in the accompanying article in this issue (Finnigan *et al.* 2015), our extensive genetic analysis of Shs1 and Cdc11 demonstrated that, once assembled onto the end of the heterooctameric rod, the salient structural element required for the physiological function of both Shs1 and Cdc11 is the portion of its C-terminal extension (CTE) that contains a sequence with the potential to form a coiled coil (CC). Prior work has shown that the CTE of Cdc11 is not essential for heterooctamer or filament formation *in vitro* (Bertin *et al.* 2008) and is not required for assembly of (or Cdc11 incorporation into) the septin superstructure at the bud neck *in vivo* (Versele *et al.* 2004). Likewise, the CTE of Shs1 is not required for its assembly into heterooctamers *in vitro* (Garcia *et al.* 2011) and, as shown in the accompanying article, not required for its incorporation into or the assembly of the septin collar *in vivo* (Finnigan *et al.* 2015). However, removal of the CTEs from both Cdc11 and Shs1, or mutational alteration of their CC elements, causes a severe growth phenotype and marked morphological elongation indicative of delayed cytokinesis arising from impaired septin function (McMurray *et al.* 2011; Finnigan *et al.* 2015). Although the CTEs of the terminal subunits could contribute to proper supramolecular organization and/or dynamics of the septin structures at the bud neck, we strongly suspected that the CTEs of these two terminal septins carry out their function, at least in part, by recruiting another cellular protein(s) via formation of a coiled-coil interaction.

In this regard, genetic or physical links between Shs1 (and/or Cdc11) and other cellular proteins that localize at the bud neck have been described, including polarisome component Spa2 (Mino *et al.* 1998), protein kinases Elm1 (Bouquin *et al.* 2000), Gin4 (Okuzaki *et al.* 1997; Mortensen *et al.* 2002), Hsl1 (Shulewitz *et al.* 1999) and Kcc4 (Barral *et al.* 1999), septin-interacting protein Nis1 (Iwase and Toh-E 2001), Myo1-binding factor Bni5 (Lee *et al.* 2002), IQGAP Iqg1 (Iwase *et al.* 2007), formin Bnr1 (Gao *et al.* 2010; Buttery *et al.* 2012), F-BAR protein Hof1 (Meitinger *et al.* 2013), and even an ER-associated protein (Scs2) (Chao *et al.* 2014). However, as described here, our genetic, biochemical, and cell biological findings demonstrate that the critical function shared by the CC elements in the CTEs of Shs1 and Cdc11 is physical association with Bni5.

Materials and Methods

Yeast strains and plasmids

Standard molecular biology techniques were used for strain and plasmid construction (Sambrook and Russell 2001). Yeast strains (Table 1) were constructed as described in detail in the accompanying article (Finnigan *et al.* 2015). In brief, the general strategy for strain construction was first to use *in vivo* ligation and homologous recombination (Muhlrad *et al.* 1992; Kitazono 2009; Bessa *et al.* 2012) to generate a *CEN* plasmid containing the gene of interest (or a corresponding gene fusion or an epitope- or fluorescent protein-tagged derivative) under the control of a promoter and terminator of choice, and harboring a juxtaposed MX-based drug cassette (Goldstein and McCusker 1999). Unless otherwise noted, the resulting construct was then amplified by PCR and integrated into a strain in which the locus of interest was marked with a different drug-resistance or nutritional marker, allowing for selection of the correct gene replacement event after transformation via the expected marker swap. If successive rounds of transformation were required, proper integration of each cassette was confirmed by multiple diagnostic PCR reactions performed on isolated genomic DNA. Because the septin genes *CDC3*, *CDC10*, *CDC11*, and *CDC12* are normally essential, alterations of the chromosomal loci for those genes were carried out in strains that contained a covering *URA3*-marked plasmid carrying the corresponding wild-type (WT) septin gene. Subsequent counterselection on an appropriate medium containing filtration-sterilized (not autoclaved) 0.5 mg/ml 5-fluoroorotic acid (5-FOA) was used to isolate derivatives that had lost the covering *URA3*-marked plasmid. Plasmids generated for this study (Table 2) were constructed by the same means described above and confirmed by DNA sequencing of the entire open-reading frame, including its junctions to both the promoter and terminator.

Culture conditions

Yeast were propagated as described in detail in the accompanying article (Finnigan *et al.* 2015). In brief, rich medium (YPD), or synthetic medium (SD) supplemented with the appropriate amino acids and/or other nutrients, contained glucose/dextrose (2%) as the carbon source. Where indicated, filtration-sterilized (not autoclaved) galactose (2%) or a raffinose (2%)-sucrose (0.2%) mixture was the carbon source. Our standard assay for assessing relative growth rates was to culture the strains of interest overnight at an appropriate temperature and then to spot fivefold serial dilutions of each strain to be tested onto agar plates, which were incubated for 2–5 days (depending on the genotypes being scored). All *cdc10Δ* strains

Table 1 Yeast strains used in this study

Genotype	Description	Reference
GFY-138[a]	BY4741; *cdc12Δ::cdc12(K392N; Δ393-407)::Hyg^R* + pJT1622	This study
GFY-104[b]	BY4741; *cdc12Δ::cdc12(K392N; Δ393-407)::mCherry::Kan^R* + pJT1622	This study
GFY-58	BY4741; *cdc11Δ::CDC11::mCherry::SpHIS5* + pJT1520	Finnigan *et al.* (2015)
GFY-122	BY4741; *cdc11Δ::cdc11(Δ357-415)::mCherry::SpHIS5* + pJT1520	Finnigan *et al.* (2015)
GFY-163	BY4741; *cdc11Δ::Kan^R shs1Δ::Hyg^R* + pJT1520	Finnigan *et al.* (2015)
GFY-121	BY4741; *cdc11Δ::cdc11(G29D)::mCherry::Kan^R* + pJT1520	Finnigan *et al.* (2015)
GFY-164	BY4741; *cdc11Δ::CDC11::mCherry::SpHIS5^R shs1Δ::Hyg^R* + pJT1520	Finnigan *et al.* (2015)
GFY-989	BY4741; *cdc11Δ::CDC11::mCherry::SpHIS5 shs1Δ::shs1(Δ349-551)::eGFP::Nat^R* + pJT1520	This study
GFY-87	BY4741; *cdc10Δ::Kan^R shs1Δ::SHS1::eGFP::Nat^R* + pJT2022	Finnigan *et al.* (2015)
GFY-137	BY4741; *cdc10Δ::Kan^R shs1Δ::Hyg^R* + pJT2022	Finnigan *et al.* (2015)
GFY-94	BY4741; *cdc10Δ::Kan^R shs1Δ::shs1(Δ349-551)::eGFP::Nat^R* + pJT2022	Finnigan *et al.* (2015)
GFY-847[c]	BY4741; *cdc11Δ::cdc11(Δ357-415)::mCherry::SpHIS5 bni5Δ::Kan^R* + pJT1520	This study
GFY-1004[a]	BY4741; *cdc12Δ::cdc12(K392N; Δ393-407)::Hyg^R bni5Δ::Kan^R* + pJT1622	This study
GFY-140	BY4741; *cdc10Δ::Hyg^R* + pJT2022	This study
GFY-1005	BY4741; *cdc10Δ::Hyg^R bni5Δ::Kan^R* + pJT2022	This study
GFY-1108	BY4741; *cdc11Δ::CDC11::mCherry::SpHIS5 shs1Δ::shs1(Δ349-551)::eGFP::Nat^R bni5Δ::Kan^R* + pJT1520	This study
GFY-846	BY4741; *cdc11Δ::CDC11::mCherry::SpHIS5^R shs1Δ::SHS1::eGFP::Nat^R bni5Δ::Kan^R* + pJT1520	This study
GFY-850	BY4741; *cdc11Δ::CDC11::mCherry::SpHIS5^R shs1Δ::Hyg^R bni5Δ::Kan^R* + pJT1520	This study
GFY-160	BY4741; *cdc11Δ::CDC11::mCherry::SpHIS5^R shs1Δ::SHS1::eGFP::Nat^R* + pJT1520	Finnigan *et al.* (2015)
GFY-540	BY4741; *cdc11Δ::cdc11(Δ357-415)::mCherry::SpHIS5 shs1Δ::shs1(1-348)::cdc11(309-415)::eGFP::Nat^R* + pJT1520	Finnigan *et al.* (2015)
GFY-1100	BY4741; *cdc11Δ::cdc11(Δ357-415)::mCherry::SpHIS5 shs1Δ::shs1(1-348)::cdc11(309-415)[d]::eGFP::Nat^R bni5Δ::Kan^R* + pJT1520	This study
GFY-542	BY4741; *cdc11Δ::cdc11(1-308)::shs1(349-551)::mCherry::Kan^R shs1Δ::shs1(Δ349-551)::eGFP::Nat^R* + pJT1520	Finnigan *et al.* (2015)
GFY-1101	BY4741; *cdc11Δ::cdc11(1-308)::shs1(349-551)::mCherry::Kan^R shs1Δ::shs1(Δ349-551)::eGFP::Nat^R bni5Δ::Kan^R* + pJT1520	This study
GFY-166	BY4741; *cdc11Δ::cdc11(Δ357-415)::mCherry::SpHIS5 shs1Δ::Hyg^R* + pJT1520	Finnigan *et al.* 2015)
GFY-1167[d]	BY4741; *cdc11Δ::cdc11(Δ357-415)::mCherry::SpHIS5 bni5Δ::HA$_3$::BNI5::Nat^R* + pJT1520	This study
GFY-1259	BY4741; *cdc11Δ::cdc11(Δ357-415)::mCherry::SpHIS5 bni5Δ::HA$_3$::bni5(Δ349-448)::Nat^R* + pJT1520	This study
GFY-1260	BY4741; *cdc11Δ::cdc11(Δ357-415)::mCherry::SpHIS5 bni5Δ::HA$_3$::bni5(Δ2-300)::Nat^R* + pJT1520	This study
GFY-1261	BY4741; *cdc11Δ::cdc11(Δ357-415)::mCherry::SpHIS5 bni5Δ::HA$_3$::bni5(Δ424-448)::Nat^R* + pJT1520	This study
GFY-1269	BY4741; *cdc11Δ::cdc11(Δ357-415)::mCherry::SpHIS5 bni5Δ::HA$_3$::bni5(Δ2-50)::Nat^R* + pJT1520	This study
GFY-1270	BY4741; *cdc11Δ::cdc11(Δ357-415)::mCherry::SpHIS5 bni5Δ::HA$_3$::bni5(Δ2-100)::Nat^R* + pJT1520	This study
GFY-1271	BY4741; *cdc11Δ::cdc11(Δ357-415)::mCherry::SpHIS5 bni5Δ::HA$_3$::bni5(Δ2-150)::Nat^R* + pJT1520	This study
GFY-1272	BY4741; *cdc11Δ::cdc11(Δ357-415)::mCherry::SpHIS5 bni5Δ::HA$_3$::bni5(Δ2-250)::Nat^R* + pJT1520	This study
GFY-1273	BY4741; *cdc11Δ::cdc11(Δ357-415)::mCherry::SpHIS5 bni5Δ::HA$_3$::bni5(Δ2-350)::Nat^R* + pJT1520	This study
GFY-1274	BY4741; *cdc11Δ::cdc11(Δ357-415)::mCherry::SpHIS5 bni5Δ::HA$_3$::bni5(Δ281-448)::Nat^R* + pJT1520	This study
GFY-1275[e]	BY4741; *cdc11Δ::cdc11(Δ357-415)::mCherry::SpHIS5 bni5Δ::HA$_3$::bni5(S270D T274D)::Nat^R* + pJT1520	This study
GFY-1276	BY4741; *cdc11Δ::cdc11(Δ357-415)::mCherry::SpHIS5 bni5Δ::HA$_3$::bni5(S346A S350A)::Nat^R* + pJT1520	This study
GFY-1277	BY4741; *cdc11Δ::cdc11(Δ357-415)::mCherry::SpHIS5 bni5Δ::HA$_3$::bni5(S346D S350D)::Nat^R* + pJT1520	This study
GFY-1278	BY4741; *cdc11Δ::cdc11(Δ357-415)::mCherry::SpHIS5 bni5Δ::HA$_3$::bni5(S270A T274A S346A S350A)::Nat^R* + pJT1520	This study
GFY-1279	BY4741; *cdc11Δ::cdc11(Δ357-415)::mCherry::SpHIS5 bni5Δ::HA$_3$::bni5(S270D T274D S346D S350D)::Nat^R* + pJT1520	This study
GFY-1286	BY4741; *cdc11Δ::cdc11(Δ357-415)::mCherry::SpHIS5 bni5Δ::HA$_3$::bni5(Δ2-200)::Nat^R* + pJT1520	This study
GFY-1287	BY4741; *cdc11Δ::cdc11(Δ357-415)::mCherry::SpHIS5 bni5Δ::HA$_3$::bni5(Δ399-448)::Nat^R* + pJT1520	This study
GFY-1288	BY4741; *cdc11Δ::cdc11(Δ357-415)::mCherry::SpHIS5 bni5Δ::HA$_3$::bni5(S270A T274A)::Nat^R* + pJT1520	This study
GFY-162	BY4741; *cdc11Δ::cdc11(Δ357-415)::mCherry::SpHIS5 shs1Δ::shs1(Δ349-551)::eGFP::Nat^R* + pJT1520	Finnigan *et al.* (2015)
GFY-573	BY4741; *cdc11Δ::cdc11(Δ357-415)::mCherry::SpHIS5 shs1Δ::shs1(Δ349-551)::BNI5::eGFP::Nat^R* + pJT1520	This study
GFY-646	BY4741; *cdc11Δ::cdc11(Δ309-415)::BNI5::mCherry::SpHIS5 shs1Δ::shs1(Δ349-551)::eGFP::Nat^R* + pJT1520	This study
GFY-579	BY4741; *cdc11Δ::cdc11(Δ357-415)::BNI5::mCherry::SpHIS5 shs1Δ::Hyg^R* + pJT1520	This study
GFY-157	BY4741; *cdc11Δ::cdc11(Δ357-415)::mCherry::SpHIS5 shs1Δ::SHS1::eGFP::Nat^R* + pJT1520	This study
GFY-911	BY4741; *cdc11Δ::cdc11(Δ357-415)::mCherry::SpHIS5 shs1Δ::SHS1::BNI5::eGFP::Nat^R* + pJT1520	This study
GFY-913	BY4741; *cdc11Δ::cdc11(Δ357-415)::mCherry::SpHIS5 shs1Δ::shs1(Δ349-551)::BNI5::eGFP::Nat^R* + pJT1520	This study
GFY-888	BY4741; *cdc11Δ::cdc11(Δ357-415)::mCherry::SpHIS5 shs1Δ::SHS1::eGFP::BNI5::Nat^R* + pJT1520	This study
GFY-890	BY4741; *cdc11Δ::cdc11(Δ357-415)::mCherry::SpHIS5 shs1Δ::shs1(Δ349-551)::eGFP::BNI5::Nat^R* + pJT1520	This study
GFY-899	BY4741; *cdc10Δ::Kan^R shs1Δ::SHS1::BNI5::eGFP::Nat^R* + pJT2022	This study

(continued)

Table 1, *continued*

Genotype	Description	Reference
GFY-901	BY4741; *cdc10Δ::Kan^R shs1Δ::shs1(Δ349-551)::BNI5::eGFP::Nat^R + pJT2022*	This study
GFY-903	BY4741; *cdc10Δ::Kan^R shs1Δ::SHS1::eGFP::BNI5::Nat^R + pJT2022*	This study
GFY-905	BY4741; *cdc10Δ::Kan^R shs1Δ::shs1(Δ349-551)::eGFP::BNI5::Nat^R + pJT2022*	This study
GFY-861	BY4741; *cdc11Δ::cdc11(Δ357-415)::mCherry::SpHIS5 shs1Δ::shs1(Δ349-551)::Nat^R + pJT1520*	This study
GFY-1295[f]	BY4741; *cdc11Δ::cdc11(Δ357-415)::mCherry::SpHIS5 shs1Δ::shs1(Δ349-551)::NanoBody::Nat^R + pJT1520*	This study
GFY-851	BY4741; *cdc11Δ::cdc11(Δ357-415)::Hyg^R shs1Δ::Nat^R + pJT1520*	This study
GFY-1291[f]	BY4741; *cdc11Δ::cdc11(Δ357-415)::NanoBody::SpHIS5 shs1Δ::Nat^R + pJT1520*	This study
GFY-1316[g]	BY4741; *CDC10::mCherry::Kan^R bni5Δ::GFP::BNI5::SpHIS5 cdc11Δ::CDC11::Hyg^R shs1Δ::shs1(Δ349-551)::Nat^R + pJT1520*	This study
GFY-1318[g]	BY4741; *CDC10::mCherry::Kan^R bni5Δ::GFP::BNI5::SpHIS5 cdc11Δ::CDC11::Hyg^R SHS1 + pJT1520*	This study
GFY-1319[g]	BY4741; *CDC10::mCherry::Kan^R bni5Δ::GFP::BNI5::SpHIS5 cdc11Δ::CDC11::Hyg^R shs1Δ::Nat^R + pJT1520*	This study
GFY-1360[g]	BY4741; *CDC10::mCherry::SpHIS5 bni5Δ::GFP::BNI5::Nat^R CDC11 shs1Δ::shs1(1-348)::cdc11(309-415)::Hyg^R*	This study
GFY-1315[g]	BY4741; *CDC10::mCherry::Kan^R bni5Δ::GFP::BNI5::SpHIS5 cdc11Δ::cdc11(Δ357-415)::Hyg^R shs1Δ::SHS1::Nat^R + pJT1520*	This study
GFY-1317[g]	BY4741; *CDC10::mCherry::Kan^R bni5Δ::GFP::BNI5::SpHIS5 cdc11Δ::cdc11(Δ357-415)::Hyg^R shs1Δ::shs1(Δ349-551)::Nat^R + pJT1520*	This study
GFY-1320[g]	BY4741; *CDC10::mCherry::Kan^R bni5Δ::GFP::BNI5::SpHIS5 cdc11Δ::cdc11(Δ357-415)::Hyg^R shs1Δ::Nat^R + pJT1520*	This study
GFY-1452[h]	*cdc10Δ::CDC10::mCherry::Hyg^R CDC11 myo1Δ::MYO1::GFP::SkHIS3 shs1Δ::Nat^R BNI5*	This study
GFY-1453[h]	*cdc10Δ::CDC10::mCherry::Hyg^R CDC11 myo1Δ::MYO1::GFP::SkHIS3 shs1Δ::SHS1::Nat^R BNI5*	This study
GFY-1454[h]	*cdc10Δ::CDC10::mCherry::Hyg^R CDC11 myo1Δ::MYO1::GFP::SkHIS3 shs1Δ::shs1(Δ349-551)::Nat^R BNI5*	This study
GFY-1456[h]	*cdc10Δ::CDC10::mCherry::Nat^R CDC11 myo1Δ::MYO1::GFP::SkHIS3 shs1Δ::shs1(1-348)::cdc11(309-415)::Hyg^R BNI5*	This study
GFY-1455[h]	*cdc10Δ::CDC10::mCherry::Kan^R CDC11 myo1Δ::MYO1::GFP::SkHIS3 shs1Δ::shs1(1-348)::cdc11(309-415)::Hyg^R bni5Δ::Nat^R*	This study
GFY-1457[h]	*cdc10Δ::CDC10::mCherry::Hyg^R CDC11 myo1Δ::MYO1::GFP::SkHIS3 shs1Δ::Nat^R bni5Δ::Kan^R*	This study
GFY-1458[h]	*cdc10Δ::CDC10::mCherry::Hyg^R CDC11 myo1Δ::MYO1::GFP::SkHIS3 shs1Δ::SHS1::Nat^R bni5Δ::Kan^R*	This study
GFY-1459[h]	*cdc10Δ::CDC10::mCherry::Hyg^R CDC11 myo1Δ::MYO1::GFP::SkHIS3 shs1Δ::shs1(Δ349-551)::Nat^R bni5Δ::Kan^R*	This study

[a] The *cdc12-6* allele, *cdc12(K391N Δ392-407)*, arises from loss of a single adenine base at position 1173; in our construct, the ORF is immediately followed by the *ADH1* transcriptional terminator sequence and a *Hyg^R* drug-resistance marker.

[b] The mCherry tag is fused in-frame after the K391N substitution within *cdc12-6*.

[c] For all yeast deleted for *BNI5*, a *bni5Δ::Kan^R* strain was first constructed by amplifying a knockout cassette PCR fragment using the *Kan^R* cassette with primer tails with homology to the immediate 5′ and 3′ UTR following the *BNI5* ORF. Subsequent deletions of *BNI5* used PCR fragments generated from this strain with ∼500 base pairs of flanking sequence.

[d] Construction of vectors containing the native *BNI5* promoter, any epitope tag or fluorescent tag, and the full-length WT *BNI5* gene resulted in extremely low plasmid yields from bacteria (TOP10 *Escherichia coli*; <5% yield compared to other vectors) using standard plasmid isolation kits. Therefore, to confirm that the desired Bni5-containing constructs had been properly generated, diagnostic PCR was first performed and then DNA sequence analysis was carried out on the PCR product (produced using a high-fidelity polymerase) containing the entire ORF including its junctions to both the promoter and terminator. The issue of low plasmid yield from bacteria did not occur for any of the truncated forms of *BNI5* or for constructs expressing *BNI5* from different promoters.

[e] A modified Quikchange PCR strategy (Zheng *et al.* 2004) was used on the gene within a TOPO-II vector prior to integration into the genome. Successive rounds of Quikchange were used to introduce multiple mutations.

[f] The 117-residue anti-GFP nanobody (sequence: MQVQLVESGGALVQPGGSLRLSCAASGFP-VNRYSMRWYRQAPGKEREWVAGMSSAGDRSSYEDSVKGRFTISRDDARNT-VYLQMNSLKP-EDTAVYYCNVNVGFEYWGQGTQVTVSSK) is derived from a single-chain *Camelidae* heavy chain antibody selected for very high affinity binding to GFP (Rothbauer *et al.* 2006; Kubala *et al.* 2010) and is encoded by a synthetic sequence using yeast codon bias (GenScript, Piscataway, NJ).

[g] The *CDC10::mCherry::Kan^R or CDC10::mCherry::SpHIS5* alleles were integrated over a WT *CDC10* by amplifying 500 nucleotides of 5′ and 3′ UTR surrounding the *CDC10* locus from genomic DNA from strain GFY-42 or GFY-1258.

[h] These strains do not contain a covering plasmid expressing any WT septin. To integrate *MYO1::GFP* at its endogenous locus, a PCR fragment containing 1183 base pairs of the C terminus of *MYO1*, the GFP tag, the *ADH1* transcriptional terminator sequence, and *SkHIS3* MX cassette, along with 1000 bases of 3′ UTR region were PCR amplified from genomic DNA (from JTY4510) and directly transformed into the appropriate strains. Integrations were confirmed using multiple diagnostic PCRs both upstream and downstream of the integrated fragment.

were grown overnight in YPGal at 22–25°. Prior to the spot tests for growth (or prior to microscopy; see next section), two successive rounds of growth at room temperature on solid medium containing 5-FOA were carried out, where indicated, to ensure removal of the covering *URA3*-marked plasmid.

Fluorescence and DIC microscopy and analysis

Cultures were grown overnight in an appropriate medium, back diluted to an $A_{600\ nm}$ ∼0.25 in rich medium (unless otherwise noted), cultured for 4–5 h to $A_{600\ nm}$ = 0.7–1.0, collected and washed by centrifugation, and samples of the resuspended cells were spotted immediately onto microscope slides. The cells were examined under a ×100 oil immersion objective using a standard upright epifluorescence microscope (model BH-2, Olympus America, Center Valley, PA) fitted with a CoolSNAP MYO CCD camera (Photometrics, Tucson, AZ) and a SOLA light engine (Lumencore, Beaverton, OR) as the light source. Images were captured using Micro-Manager software

Table 2 Plasmids used in this study

Plasmid	Description	Reference
pSB1/JT1520	pRS316 *URA3 CDC11*	Versele *et al.* (2004)
pMVB57/JT2022	YCplac33 *URA3 CDC10*	McMurray *et al.* (2011)
pMVB39/JT1622	YCplac33 *URA3 CDC12*	Versele and Thorner (2004)
pGF-V68[a]	pRS315 *prSHS1::SHS1*	This study
pGF-IVL1	pRS315 *prCDC11::CDC11::mCherry::SpHIS5*	Finnigan *et al.* (2015)
pRS315	*CEN, LEU2*	Sikorski and Hieter (1989)
pGF-preIVL6	pRS315 *prCDC10::CDC10::mCherry::SpHIS5*	Finnigan *et al.* (2015)
pGF-IVLBNI5[b]	pRS315 *prGAL1/10::BNI5::eGFP::SpHIS5*	This study
pGF-IVL384	pRS315 *prSHS1::BNI5::eGFP::Nat^R*	This study
pGF-IVL385	pRS315 *prCDC11::BNI5::eGFP::Nat^R*	This study
pGF-IVL414	pRS315 *prGAL1/10::bni5(Δ2-50)::eGFP::SpHIS5*	This study
pGF-IVL415	pRS315 *prGAL1/10::bni5(Δ2-100)::eGFP::SpHIS5*	This study
pGF-IVL416	pRS315 *prGAL1/10::bni5(Δ2-150)::eGFP::SpHIS5*	This study
pGF-IVL429	pRS315 *prGAL1/10::bni5(Δ2-200)::eGFP::SpHIS5*	This study
pGF-IVL430	pRS315 *prGAL1/10::bni5(Δ2-250)::eGFP::SpHIS5*	This study
pGF-IVL431	pRS315 *prGAL1/10::bni5(Δ2-300)::eGFP::SpHIS5*	This study
pGF-IVL432	pRS315 *prGAL1/10::bni5(Δ2-350)::eGFP::SpHIS5*	This study
pGF-IVL433	pRS315 *prGAL1/10::bni5(Δ424-448)::eGFP::SpHIS5*	This study
pGF-IVL417	pRS315 *prGAL1/10::bni5(Δ399-448)::eGFP::SpHIS5*	This study
pGF-IVL418	pRS315 *prGAL1/10::bni5(Δ349-449)::eGFP::SpHIS5*	This study
pGF-IVL419	pRS315 *prGAL1/10::bni5(Δ281-448)::eGFP::SpHIS5*	This study
pGF-IVL448[c]	pRS315 *prGAL1/10::bni5(S270A T274A)::eGFP::SpHIS5*	This study
pGF-IVL449	pRS315 *prGAL1/10::bni5(S270D T274D)::eGFP::SpHIS5*	This study
pGF-IVL450	pRS315 *prGAL1/10::bni5(S346A S350A)::eGFP::SpHIS5*	This study
pGF-IVL451	pRS315 *prGAL1/10::bni5(S346D S350D)::eGFP::SpHIS5*	This study
pGF-IVL452	pRS315 *prGAL1/10::bni5(S270A T274A S346A S350A)::eGFP::SpHIS5*	This study
pGF-IVL453	pRS315 *prGAL1/10::bni5(S270D T274D S346D S350D)::eGFP::SpHIS5*	This study
pGF-IVL255	pRS315 *CDC10::BNI5::mCherry::SpHIS5*	This study
pGF-IVL216	pRS315 *prCDC11::GFP::Kan^R*	This study
pGF-IVL585	pRS315 *prBNI5::BNI5::GFP::SpHIS5*	This study
pGF-IVL473	pRS315 *prBNI5::HA$_3$::BNI5::Nat^R*	This study
pGF-IVL425	pRS315 *prMYO1::MYO1::GFP::Kan^R*	This study
pGF-IVL553	pRS315 *prNIS1::NIS1::GFP::Kan^R*	This study
pGF-IVL559	pRS315 *prSYP1::SYP1::GFP::Kan^R*	This study

[a] The *SHS1* gene has ~500 nucleotides of the native promoter and terminator sequence PCR amplified from BY4741.

[b] For vectors overexpressing *BNI5*, a modified *in vivo* ligation protocol was used that first constructed a vector (pGF-IVL300) linking the *GAL1/10* promoter (814 base pairs) with the *ADH1(t)::SpHIS5* cassette separated by a unique *Not*I restriction site. Following digestion to gap the vector, the *BNI5* gene was amplified with homology to the promoter and terminator sequence and cotransformed into yeast. This strategy does not include a selectable marker on one of the PCR fragments, but rather, selects for recircularization of the plasmid (on medium lacking leucine).

[c] Ala substitutions for Ser and Thr residues were constructed within a TOPO II + *BNI5* vector (pGF-V389) prior to PCR amplification for *in vivo* ligation and homologous recombination.

(Edelstein *et al.* 2010) and adjusted using ImageJ [National Institutes of Health (NIH), Bethesda, MD] and Photoshop (Adobe, San Francisco). In any given experiment, all the images were scaled, adjusted for brightness (where necessary), and resized identically. To determine the periphery of the cell, either an overexposed image or a DIC image was used.

For quantification of cell morphology, experiments were performed in triplicate and, in any given experiment, 50–200 cells in multiple fields of view were examined for each genotype. Values presented are the absolute population percentages; error represents standard deviation of the mean value. For quantification of fluorescence intensity using ImageJ, the GFP signal at the bud neck was captured (with the box tool) and the cytosolic GFP signal was assessed (with the line tool) by a cross-section across the midpoint of the cell (either a mother or a daughter). The bud neck and cytosolic signals were measured for ~100 cells of each genotype, and average pixel intensity at each location was determined after subtracting the average background fluorescence from five random regions of the image not containing any cells. For clarity, pixel intensity values are presented as relative to WT control strain (set at 100%). In general, statistical significance was assessed using an unpaired *t*-test, and *P*-values were all <0.05 (unless otherwise noted). To compare the statistical significance of the morphology differences observed among the different genotypes and conditions graphically depicted in Figure 1C, a two-way ANOVA and multiple comparison analysis with a Bonferroni correction (Statistics Toolbox, Matlab 2013, Mathworks, Natick, MA) was performed.

Results

Overexpression of Bni5 suppresses the growth and morphology defects of CTE-less Cdc11 and Shs1 mutants

Our accompanying study (Finnigan *et al.* 2015) demonstrated that the CTEs of Cdc11 and Shs1 are critical for full septin

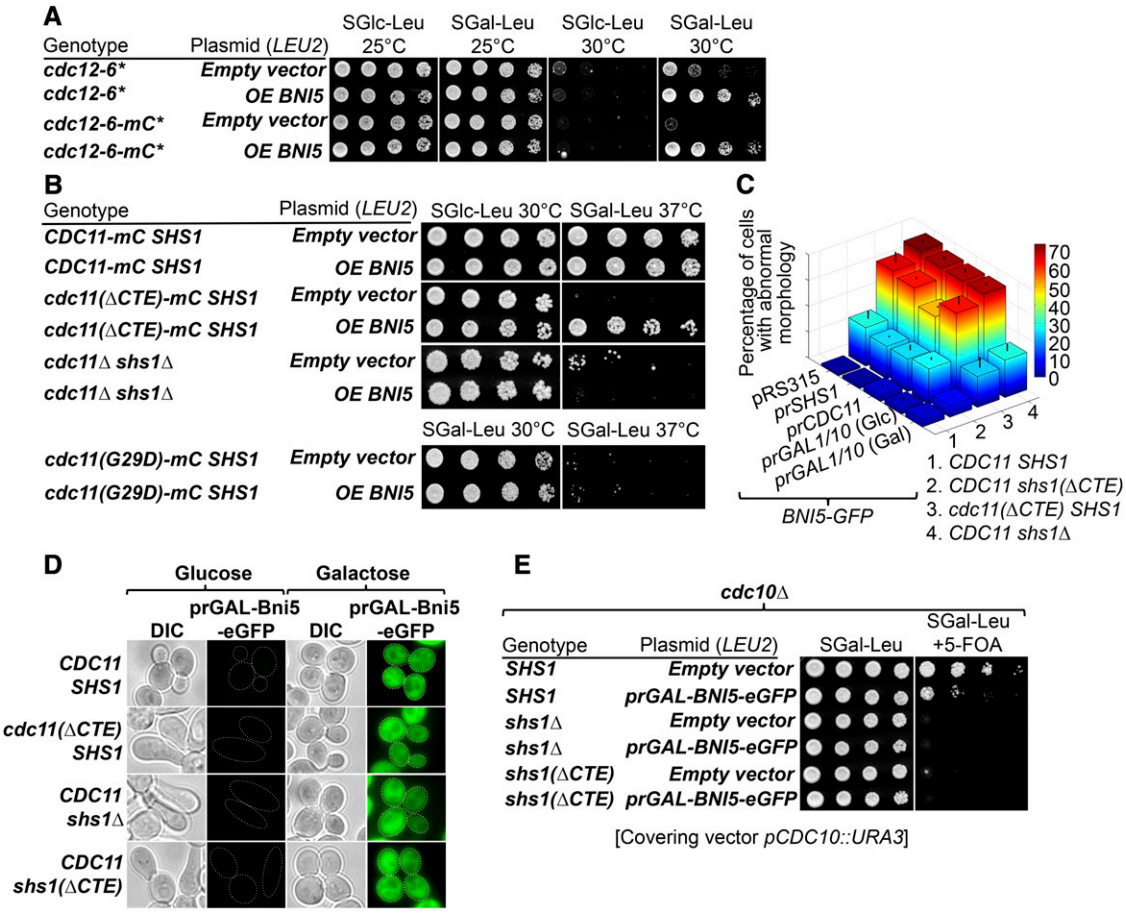

Figure 1 Bni5 is a potent dosage suppressor of CTE-less Cdc11 and Shs1 mutants. (A) Strains GFY-138 and GFY-104 expressing from the endogenous *CDC12* locus the product of the *cdc12-6* frameshift allele, Cdc12(K392N Δ393-407), either alone or C-terminally tagged with mCherry (mC), were transformed with either empty vector (pRS315) or the same vector expressing Bni5-eGFP under control of the *GAL1/10* promoter (pGF-IVLBNI5). Asterisk, indicates that an *ADH1* transcriptional terminator::*Hyg*^{R} cassette was inserted directly after the ORF. After selection on medium containing 5-FOA to remove the covering *URA3*-marked CDC12-expressing plasmid, the cells were propagated overnight in YPRaf-Suc medium at 25°, spotted onto solid medium containing either glucose (Glc) or galactose (Gal) as the carbon source, as indicated, and incubated at the indicated temperature. (B) As in A, GFY-58, GFY-122, GFY-163, and GFY-121 were transformed with either empty vector or the same vector expressing *GAL* promoter-driven Bni5-eGFP. Just prior to testing, the cells were selected twice on SD −Leu medium containing 5-FOA to remove the covering *URA3*-marked *CDC11*-expressing plasmid, propagated overnight in YPRaf-Suc at 25°, then spotted onto medium containing Glc or Gal (top three panels) or on SGal −Leu at 30° or 37° (bottom panel). (C) GFY-58 (1), GFY-122 (2), GFY-164 (3), and GFY-989 (4) were transformed with empty vector control (pRS315) or derivatives of the same vector expressing Bni5-eGFP from the *SHS1* promoter (pGF-IVL384), the *CDC11* promoter (pGF-IVL385), or the *GAL1/10* promoter (pGF-IVLBNI5). After removal of the covering *URA3*-marked *CDC11*-expressing plasmid, as in B, cells were grown at 30° in the appropriate medium to midexponential phase, and then triplicate samples (each 50–150 cells) were analyzed by fluorescence and DIC microscopy. The percentage of cells with an abnormal morphology is plotted as a three-dimensional heat map (error represents standard deviation of the mean). For all four strains (1–4), only high-level GAL promoter-driven expression of Bni5-eGFP was able to effect restoration of normal morphology in a statistically significant ($P << 0.05$) manner, as judged by a two-way ANOVA and multiple comparison analysis. (D) Representative images of samples of the indicated cultures from C visualized by fluorescence and DIC microscopy. Exposure time for Glc-grown cells was three times longer than for Gal-grown cells to verify lack of detectable Bni5-eGFP expression. Dotted white line, cell periphery. (E) GFY-87, GFY-137, and GFY-94 were transformed with empty vector (pRS315) or the same vector expressing Bni5-eGFP under *GAL1/10* promoter control (pGF-IVLBNI5) and propagated on SD −Ura −Leu medium, then grown overnight in YPGal at 25° prior to spotting onto Gal medium without or with 5-FOA to remove the covering *URA3*-marked *CDC10*-expressing plasmid. The same test was repeated using overnight culture in SGal −Leu to maintain selection for the *LEU2*-marked plasmid and yielded the same results (data not shown).

function *in vivo*. Yet, the combined contributions of these structural elements remained elusive. However, given that the potential CC-forming residues are the essential sequence feature required for their function (Finnigan *et al.* 2015), we suspected that these CTEs associate with and thereby recruit to the septin superstructure additional cellular factors that must execute their physiological role at the bud neck. As a first means to explore this possibility, and to approach this question in as unbiased a manner as possible, we cataloged all of the nonseptin gene products reputed to be localized to the yeast bud neck during the time in the cell cycle when the septin collar is present (Gladfelter *et al.* 2001; Kumar *et al.* 2002; Huh *et al.* 2003), but restricted our analysis to those that met both of two additional criteria: (i) bud neck

Table 3 Bud neck-localized and/or septin collar-associated proteins

Gene product	OE[a]	Deletion	Paralog	Apparent function	Reference
Axl2/Bud10	3	Viable	—	Cadherin-like plasma membrane glycoprotein	Gao *et al.* (2007)
Bem2	1	Viable	—	Rho4 GTPase-activating protein	Gong *et al.* (2013)
Bil1	0	Viable	—	Bud6-associated factor involved in Bnr1-dependent actin cable assembly	Graziano *et al.* (2013)
Bni1	0	Viable	Bnr1	Formin that catalyzes actin cable assembly	Buttery *et al.* (2007)
Bni4	1	Viable	—	Targeting subunit for Glc7 (phosphoprotein phosphatase 1 catalytic subunit)	Kozubowski *et al.* (2003)
Bni5	0	Viable	—	Myo1 (type II myosin)-binding factor	Fang *et al.* (2010)
Bnr1	3	Viable	Bni1	Formin that catalyzes actin cable assembly	Buttery *et al.* (2012)
Bud3	1	Viable	—	Cdc42 guanine nucleotide exchange factor (GEF)	Kang *et al.* (2014)
Bud4	1	Viable	—	Annillin-like protein	Wu *et al.* (2015)
Bud6/Aip3	0	Viable	—	Nucleation-promoting factor (NPF) for formin Bni1	Tu *et al.* (2012)
Cdc5	3	Inviable	—	Polo family protein kinase	Sakchaisri *et al.* (2004)
Chs7	1	Viable	—	Chaperone/escort factor for export of Chs3 (chitin synthase III catalytic subunit) from the ER	Kota and Ljungdahl (2005)
Cla4	1	Viable	Skm1	Cdc42-activated, PAK family protein kinase	Versele and Thorner (2004)
Dbf4	0	Inviable	—	Regulatory subunit of protein kinase Cdc7	Hoang *et al.* (2007)
Elm1	1	Viable	—	LKB1 family protein kinase	Asano *et al.* (2006)
Gic2	3	Viable	Gic1	Cdc42-binding and Bni1-interacting protein	Chen *et al.* (2012)
Gin4	1	Viable	Kcc4	AMPK-like family protein kinase	Roelants *et al.* (2015)
Hof1/Cyk2	3	Viable	—	F-BAR- and SH3 domain-containing protein involved in actomyosin ring dynamics	Meitinger *et al.* (2013)
Hsl1	3	Viable	—	AMPK-like family protein kinase	Crutchley *et al.* (2009)
Iqg1/Cyk1	3	Inviable	—	An actin-, Cmd1 (calmodulin), and Cdc42-binding IQGAP1-related protein involved in actomyosin ring dynamics	Tian *et al.* (2014)
Kcc4	1	Viable	Gin4	AMPK-like family protein kinase	Okuzaki *et al.* (2003)
Mlc2	0	Viable	—	Regulatory light chain for Myo1	Tully *et al.* (2009)
Myo1	3	Inviable	—	Type II myosin in cytokinetic actomyosin ring	Wloka *et al.* (2013)
Nba1	0	Viable	—	Nap1 (histone chaperone)-associated protein and Cdc42 antagonist	Meitinger *et al.* (2014)
Nis1	0	Viable	—	Component of the Ris1-containing SUMO-targeted ubiquitin ligase (STubL)	Alonso *et al.* (2012)
Rga1	1	Viable	Rga2	Cdc42 GTPase-activating protein	Smith *et al.* (2002)
Rgd1	2	Viable	—	Rho3 and Rho4 GTPase-activating protein	Claret *et al.* (2005)
Skt5/Chs4	1	Viable	Shc1	Bni4-interacting Chs3 activator	Ono *et al.* (2000)
Svl3	0	Viable	Pam1	Maybe involved in pantothenate metabolism	Zheng *et al.* (1998)

[a] Summary of the severity of the effect on apparent growth rate caused by overexpression of the indicated gene product, based on prior published studies: 0, no detectably deleterious effect; 1, only a mild/slight decrease in growth rate; 2, a moderate decrease in growth rate; and 3, a severe inhibition of growth. The three most comprehensive studies (Sopko *et al.* 2006; Yoshikawa *et al.* 2011; Makanae *et al.* 2013) are generally, but not always, in agreement. Moreover, cross-comparisons among these datasets is complicated by the fact that the constructs, conditions, and protocols employed to test the effect of overexpression were not uniform. For example, although two genome-wide analyses used induction from a *GAL* promoter to drive overexpression (Sopko *et al.* 2006; Yoshikawa *et al.* 2011), they differed in whether the vector was a *CEN* or a 2-μm DNA plasmid, whether the gene product was tagged or not, the nature of the tag, etc.; and, in the third global analysis, the native gene and its promoter were used and overexpression was achieved solely by the use of a high-copy-number vector (Makanae *et al.* 2013). Data for the following genes are derived from other studies where, in some cases, assessing the effect of overexpression was not a primary goal of the investigators: Bem2 (Knaus *et al.* 2007), Bni4 (Stevenson *et al.* 2001), Bnr1 (Kikyo *et al.* 1999), Cdc5 (Kitada *et al.* 1993), Elm1 (Moriya and Isono 1999), and Kcc4 (Okuzaki *et al.* 2003).

localization has been thoroughly documented by independent means; and, (ii) where tested, recruitment to the bud neck is septin dependent (*i.e.*, bud neck localization is eliminated upon disassembly of the septin collar in *cdc12-6*^{ts} mutants shifted to restrictive temperature). This bioinformatic analysis yielded nearly 30 gene products (Table 3).

Each of the corresponding genes was tagged in-frame at its C-terminal end with eGFP and the resulting derivative cloned into the same *LEU2*-marked *CEN* vector (pRS315) under *GAL* promoter control. We reasoned that, given the very high level of expression achievable from the *GAL* promoter (Mumberg *et al.* 1994), the factor normally recruited to the bud neck region via its association with the CTEs of Cdc11 and Shs1 would populate the bud neck region at a sufficient level after Gal induction to achieve detectable rescue of the growth debility of cells in which both CTEs were lacking. Indeed, using this very stringent condition, only overexpression of Bni5 gave robust restoration of growth in both *cdc11(ΔCTE) shs1(ΔCTE)* and *cdc11(ΔCTE) shs1Δ* cells (Supporting Information, Table S3).

BNI5 was originally characterized as a multicopy suppressor of the temperature sensitivity of a *cdc12-6* mutant (Lee *et al.* 2002). As an independent means to demonstrate that our *BNI5* overexpression construct was behaving properly, we tested whether it was also able to restore growth to *cdc12-6*^{ts} cells at the restrictive temperature. Reassuringly, upon Gal induction, our Bni5-GFP construct efficiently suppressed the *ts* phenotype of *cdc12-6* cells (Figure 1A).

To confirm that the Bni5-mediated growth suppression is exerted through either Shs1 or Cdc11, and requires that at least one of these terminal septin subunits have an intact CTE, we conducted the following tests. First, we found that overexpression of Bni5 had no deleterious effect on wild-type cells (Figure 1B, top panel) and, most tellingly, was able to rescue the growth of cells in which only Shs1 has an intact CTE (Figure 1B, second panel). This suppression of *cdc11(ΔCTE)* cells was specific because Bni5 overexpression was unable to improve the growth of cells lacking both Cdc11 and Shs1 (Figure 1B, third panel) and was unable to rescue growth of cells in which the defect in Cdc11 is inability to form a proper G interface with Cdc12, the penultimate subunit in the heterooctamer (Figure 1B, bottom panel). Conversely, and as judged by the independent criterion of morphology, *GAL* promoter-driven expression of Bni5 was able to suppress the elongated bud phenotype of cells in which only Cdc11 has an intact CTE (Figure 1C, rows 2 and 4; Figure 1D, two lowermost panels), just as efficiently as in cells in which only Shs1 has an intact CTE (Figure 1C, row 3; Figure 1D, second panel from the top). The observed reductions in the percentage of cells displaying abnormal morphology upon Bni5 overexpression were all reproducible and statistically significant ($P << 0.05$).

It has been observed previously by us (McMurray *et al.* 2011) and others (Iwase *et al.* 2007) that an *shs1Δ cdc10Δ* double mutant is inviable. In keeping with our other evidence that the CTE of Shs1 is essential for its function (Finnigan *et al.* 2015), we found that, like a complete *shs1Δ* null allele, a *shs1(ΔCTE)* mutant was unable to support the growth of *cdc10Δ* cells and was unable to support rescue by *BNI5* overexpression (Figure 1E).

Loss of Bni5 phenocopies the growth and morphology defects of CTE-less Shs1 and Cdc11 mutants

Cumulative evidence indicates that Bni5 is a septin-associated protein (Lee *et al.* 2002) and that it has a role in localizing Myo1 to the bud neck prior to the onset of cytokinesis (Fang *et al.* 2010; Schneider *et al.* 2013). However, how Bni5 is recruited to the septin collar has been unclear.

As described in the accompanying article (Finnigan *et al.* 2015), we established four different backgrounds in which expression of *SHS1* is required for cell viability. One of these conditions is in cells lacking Hof1, a bud neck-localized, F-BAR- and SH3 domain-containing protein that contributes to regulating actomyosin ring dynamics (Nishihama *et al.* 2009; Meitinger *et al.* 2011). Similarly, it has been reported that a *bni5Δ hof1Δ* double mutant is inviable (Nam *et al.* 2007a). Hence, we tested whether loss of Bni5 also exacerbated the growth phenotype in our three other Shs1-dependent strain backgrounds. Like loss of Shs1 itself, absence of Bni5 was lethal in cells expressing Cdc11(ΔCTE)-mC and in *cdc10Δ* cells, and severely compromised growth in *cdc12-6* cells even at permissive temperature (Figure 2A). Thus, the effects on growth of a *bni5Δ* mutation mirror those of an *shs1Δ* mutation, strongly connecting the functions of these two proteins.

In agreement with this conclusion, and as judged by the independent criterion of morphology, in cells expressing Cdc11-mC as the sole source of this septin (which sensitizes cells to the loss of Shs1) (Finnigan *et al.* 2015), we found that absence of either Shs1 or its CTE yielded a marked increase in the percentage of cells in the population with a dramatically elongated morphology that was at least as dramatic as loss of Bni5 itself (Figure 2B, compare columns 2 and 3 to 5) and the effect of loss of both Bni5 and Shs1 was not more severe than loss of Shs1 alone (Figure 2B, compare columns 2 and 6). However, complete absence of Shs1 caused a more pronounced effect than removal of its CTE alone (Figure 2B, compare columns 2 and 3), indicating that the globular GTP-binding domain of Shs1 contributes to Shs1 function independent from its CTE. As data provided in the accompanying article argue (Finnigan *et al.* 2015), at the septin collar, Shs1-capped heterooctamers likely form heterotypic end-to-end NC junctions with Cdc11-capped heterooctamers. Hence, in the complete absence of Shs1, Cdc11 cannot be properly positioned, whereas in cells expressing Shs1(ΔCTE), it can. As the accompanying article also demonstrates, the CTEs of Shs1 and Cdc11 have a function in common. Taken together, these considerations suggest that, in Shs1(ΔCTE) cells, the CTE in Cdc11 can act in lieu of the CTE of Shs1. If this shared function is recruitment of Bni5 to the bud neck, then loss of Bni5 should enhance the phenotype of Shs1(ΔCTE) cells, as we indeed observed (Figure 2B, compare columns 3 and 4).

To confirm more directly the link between the CTEs of Shs1 and Cdc11 and Bni5 function, we took advantage of chimeras in which we swapped the CTEs of Cdc11 and Shs1 that, as demonstrated in the accompanying article, are functional when present as the sole source of a CTE on a terminal septin subunit (Finnigan *et al.* 2015). When cells possess the native CTEs of both Cdc11 and Shs1 (Figure 2C, top row) or just the native CTE of Shs1 (Figure 2A, top row), they are fully viable. However, if the native CTEs of both Cdc11 and Shs1 are removed, the cells are inviable, even though Bni5 is present. By contrast, if the Cdc11 CTE is appended to Shs1 in place of its endogenous CTE, robust growth is restored (Figure 2C, row 3); however, that growth is markedly compromised when Bni5 is absent (Figure 2C, row 4). Even more strikingly, if the Shs1 CTE is appended to Cdc11 in place of its endogenous CTE, growth is also restored (Figure 2C, row 5) and their abiity to grow is completely dependent on the presence of Bni5 (Figure 2C, row 6). Also, in both Cdc11(ΔCTE) Shs1(ΔCTE)-CTE^{Cdc11} and Cdc11(ΔCTE)-CTE^{Shs1} Shs1(ΔCTE) cells, loss of Bni5 further exacerbated their morphological phenotype (Figure 2D). Thus, even when operating "in *trans*," the function of CTEs of Cdc11 and Shs are dependent on Bni5.

If Bni5 action is mediated largely via its interaction with the CTEs of Cdc11 and Shs1, when both the Cdc11 and Shs1 CTEs are absent, then removal of Bni5 should have little or

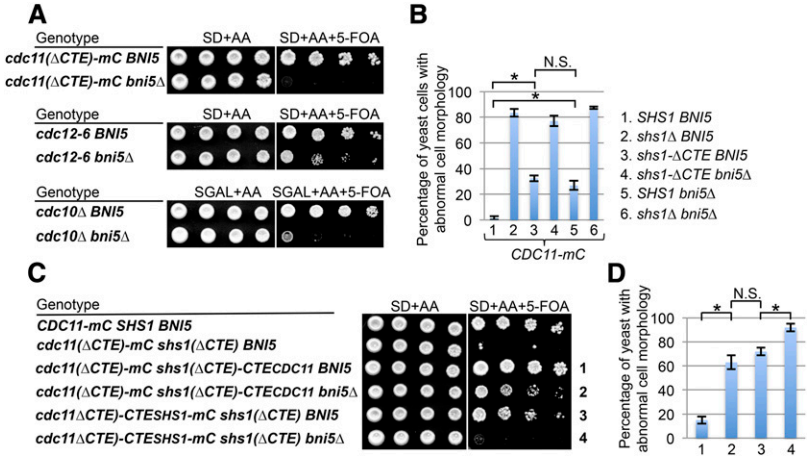

Figure 2 Loss of *BNI5* mimics loss of *SHS1*. (A) Strains GFY-122 and GFY-847 (upper panel) and GFY-138 and GFY-1004 (middle panel) were grown overnight in SD −Ura medium at 30° and then spotted onto control medium lacking 5-FOA (left) or the same medium containing 5-FOA to select against, respectively, the covering *URA3*-marked *CDC11*- or *CDC12*-expressing plasmid, and incubated for 3 days. GFY-140 and GFY-1005 (lower panel) were incubated overnight in YPGal medium at 25° and spotted onto Gal medium without or with 5-FOA (to select against the covering *URA3*-marked *CDC10*-expressing plasmid) and grown at room temperature for 5 days. (B) Triplicate samples of exponentially growing cultures of GFY-58, GFY-164, GFY-989, GFY-1108, GFY-846, and GFY-850 grown at 30° were viewed by DIC microscopy to examine the morphology of the corresponding cells (100–200 total) after selection on medium containing 5-FOA to remove the covering *URA3*-marked *CDC11*-expressing plasmid. Values represent the percentage of cells in the population with abnormal morphology (error is standard deviation of the mean). Asterisk, difference is statistically significant ($P < 0.05$), as judged by an unpaired *t*-test; N.S., no statistically significant difference. (C) Growth of GFY-160, GFY-162, GFY-540, GFY-1100, GFY-542, and GFY-1101 was assessed before and after removal of the covering *URA3*-marked *CDC11*-expressing plasmid, as in A, upper panel. (D) Morphology of the cells in triplicate samples of the strains in C was quantified as in B.

no additional effect. Indeed, we found that deletion of *BNI5* conferred only a very subtle enhancement of the deleterious growth phenotype of *cdc11(ΔCTE) shs1(ΔCTE*) cells (Figure S1A). Collectively, our findings provide a strong genetic link between the CTEs of Cdc11 and Shs1.

To begin to address whether this link is also physical, we examined the efficiency of recruitment to the bud neck of endogenously expressed eGFP-Bni5, and found that, compared to the WT control, there was a marked reduction in the fluoresence intensity at the bud neck in *cdc11(ΔCTE) shs1(ΔCTE*) cells (Figure S1B, left). Concomitant with the substantially diminished signal at the septin collar (Figure S1B, middle), there was an increase in cytosolic fluorescence (Figure S1B, right). These observations demonstrate that the CTEs of Cdc11 and Shs1 make a significant, but not the sole, contribution to efficient recruitment of Bni5 to the septin collar, as we further confirmed (see Figure 6). Given that we have found that septin heterooctamers cannot be assembled *in vitro* in the absence of Cdc10 (Bertin *et al.* 2008) and that *in vivo* the resulting Cdc11-Cdc12-Cdc3 and/or Shs1-Cdc12-Cdc3 trimers associate only very inefficiently to form heterohexamers (via an atypical Cdc3-Cdc3 G interface-mediated interaction) (McMurray *et al.* 2011), we suspect that the observed inability of overexpressed Bni5 to suppress the *shs1(ΔCTE)* allele in *cdc10Δ* cells (Figure 1E) is due to gross aberrations in septin superstructure.

Only the C-terminal third of Bni5 is required for its function

Using the most sophisticated modeling program available (Phyre[2]) (Kelley and Sternberg 2009), Bni5 is predicted to be a remarkably elongated and nearly all α-helical protein (Figure S2A), consistent with the possibility that it could associate with the CC elements in the CTEs of Cdc11 and Shs1 via a coiled-coil interaction. To date, no study has investigated what portions of the Bni5 protein are required for its ability to interact with septins or to suppress septin defects when overexpressed. Therefore, we generated a nested series of both N- and C-terminal truncations, each tagged at its C terminus with GFP (Figure S2B). Each of these truncations was inserted into the same *LEU2*-marked vector under the control of the *GAL* promoter (pGF-IVLBNI5) and its ability to rescue the growth of *cdc11(ΔCTE)* cells at 37° was assessed exactly as described in Figure 1B. The results of this analysis were clear cut (data not shown) and are summarized in Figure 3A. Potent suppression was observed even with truncations that removed the first 300 residues of the protein; conversely, removal of as few as 25 residues from the C terminus crippled the suppression and removal of 50 residues totally abrogated the ability of the overproduced protein to support the growth of *cdc11(ΔCTE)* cells at 37°. Also, a prior study claimed that cell-cycle dependent phosphoregulation of Bni5 at four sites (S270, T274, S346, and S350) is important for its cellular function (Nam *et al.* 2007a). Hence, we mutated full-length GFP-tagged Bni5 at pairs of these sites or at all four sites to generate both non-phosphorylatable alleles (S270A T274A, S346A S350A, and S270A T274A S346A S350A) and phosphomimetic alleles (S270D T274D, S346D S350D, and S270D T274D S346D S350D). All six of these Bni5 mutants were able to suppress the growth of *cdc11(ΔCTE)* cells at 37° as robustly as WT Bni5, as summarized in Figure 3A.

As we showed, growth of *cdc11(ΔCTE)-mC* cells is totally dependent on endogeneous Shs1 (Finnigan *et al.* 2015). Likewise, growth of *cdc11(ΔCTE)-mC* cells is totally dependent on endogenous Bni5 (Figure 2A and Figure 3A, top). Therefore, to confirm our findings about Bni5 derived from overexpression of the truncated alleles, we retested the entire deletion set by integrating the same constructs, each tagged at is N terminus with a $(HA)_3$ tag, into the *BNI5* locus under control of the native *BNI5* promoter. We demonstrated, first, that the N-terminal $(HA)_3$ tag does not deleteriously affect

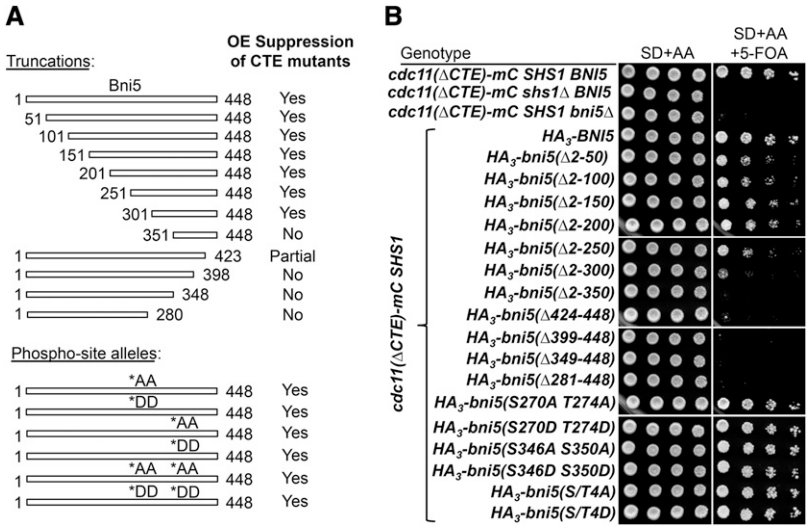

Figure 3 Mutational analysis of Bni5. (A, upper panel) Summary of the ability of a plasmid expressing full-length Bni5-eGFP (pGF-IVLBNI5) or the indicated derived series of nested N-terminal (pGF-IVL414 through pGF-IVL416) and C-terminal (pGF-IVL429 through pGF-IVL433) truncation mutants, each eGFP tagged and expressed from the *GAL* promoter on the same *CEN* vector (pRS315), to suppress the growth defect of *cdc11(ΔCTE) SHS1* cells (GFY-122), when overexpressed on Gal medium, as assessed in Figure 1B. Numbers indicate the residues of Bni5 present in each construct. (Lower panel) The ability of the indicated nonphosphorylatable (A, Ala) and phosphomimetic (D, Asp) Bni5 substitution mutations of Ser and/or Thr at positions 270, 274, 346, and 350 (pGF-IVL417 to pGF-IVL419 and pGF-IVL448 to pGF-IVL453), to suppress the growth of GFY-122 was assessed in the same way. In brief, each plasmid-containing transformant of GFY-122 was propagated as a single clonal isolate on medium containing 5-FOA to select for loss of the covering *URA3*-marked *CDC11*-expressing plasmid, then reselected on 5-FOA medium a second time, grown overnight in SRaf/Suc −Leu at 25°, then serially diluted and spotted on either SD −Leu or SGal −Leu medium. Growth was scored after incubation at 37° for 2 days. Yes, robust growth observed only on Gal medium; partial, weak growth observed only on Gal medium; no, no detectable growth observed on Gal medium, *i.e.*, indistinguishable from the lack of growth on Gal medium of GFY-122 cells carrying the empty (control) vector, pRS315. (B) The ability of the indicated Bni5 derivatives, each fused to an N-terminal 3XHA tag and integrated into and expressed from the native *BNI5* locus on chromosome XIV (strains GFY-122, GFY-166, GFY-847, GFY-1167, GFY-1259 through GFY-1261, GFY-1269 through GFY-1279, and GFY-1286 through GFY-1288), to complement the inviability of *cdc11(ΔCTE)-mC SHS1 bni5Δ* cells, was assessed after growth overnight at 30° and then spotting onto control medium or the same medium containing 5-FOA to select against the covering *URA3*-marked *CDC11*-expressing plasmid.

Bni5 function (Figure S3A). We then determined whether each Bni5 mutant expressed at its endogenous level was able to support the growth of *cdc11(ΔCTE)-mC* cells when the covering *CDC11*-expressing plasmid was removed. We found again that function was preserved even when as many as 200 to 250 N-terminal residues were removed and slight growth was still detectable even when 300 N-terminal residues were removed, whereas Bni5 function was completely eliminated by removal of as few as 25 C-terminal residues. Likewise, none of the three nonphosphorylatable alleles and none of the phosphomimetic alleles has any detectably deleterious effect on Bni5 function. Thus, analysis of functional domains in Bni5 by two independent approaches led to the same conclusion, namely its C-terminal end is critical for its physiological function. Consistent with this finding, the 90 or so C-terminalmost residues are the most highly conversed region in Bni5 (Figure S2B).

Fusion of Bni5 obviates the need for the CTEs of Shs1 and Cdc11

If the primary role of the CTEs of Shs1 and Cdc11 is to anchor Bni5 at their location in the bud neck, we reasoned that chimeric proteins, in which Bni5 itself replaced the CTEs of these two terminal septin subunits, might rescue the inviability of *cdc11(ΔCTE) shs1(ΔCTE)* cells. Therefore, we constructed the corresponding translational fusions wherein Bni5 was attached in-frame to the C terminus of CTE-less Shs1 and CTE-less Cdc11. We found that replacement of the CTE of Shs1 with Bni5 (tagged at its C terminus with eGFP) was able to robustly support the growth of *cdc11(ΔCTE) shs1(ΔCTE)* cells (Figure 4A, compare lanes 2 and 3). This result was all the more striking because we had found that Bni5 tagged at its C terminus was somewhat compromised for function, compared to Bni5 tagged at its N terminus (Figure S3A), although, in the context of fusion to Shs1(ΔCTE), either orientation (eGFP-Bni5 or Bni5-eGFP) supported growth equally well (Figure 4B) and were efficiently incorporated into the septin collar at the bud neck (Figure 4C). We noted, however, that fusion of either eGFP-Bni5 or Bni5-eGFP to full-length Shs1 gave detectably better growth than when fused to Shs1(ΔCTE). One possibility for the slight growth advantage of the former is that it should be capable of recruiting additional Bni5 via its CTE. However, the same slight growth advantage of Shs1-Bni5 constructs over Shs1(ΔCTE)-Bni5 constructs (regardless of whether Bni5 was tagged at it N- or C-terminal end with eGFP) was observed in the presence or absence of endogenous *BNI5* (Figure S4).

Like the inability of Bni5 overexpression to rescue the growth of *shs1(ΔCTE)* in *cdc10Δ* cells (Figure 1E), fusion of Bni5 to Shs1(ΔCTE) was not sufficient to restore Shs1 function in cells lacking Cdc10 (Figure 4D). Moreover, unlike fusions of Bni5 to Shs1 (Figure 4, A and B), fusion of Bni5 to the Cdc10 subunit was unable to rescue the lethality of *cdc11(ΔCTE) shs1(ΔCTE)* cells (Figure 4E).

Increased conformational flexibility enhances Bni5-mediated rescue of CTE-less Shs1 and Cdc11

Strikingly, unlike fusion of Bni5 to Shs1(ΔCTE), fusion of Bni5 to Cdc11(ΔCTE) was unable to restore growth to *cdc11(ΔCTE) shs1(ΔCTE)* cells (Figure 4A), even though the chimeric constructs also were efficiently expressed and

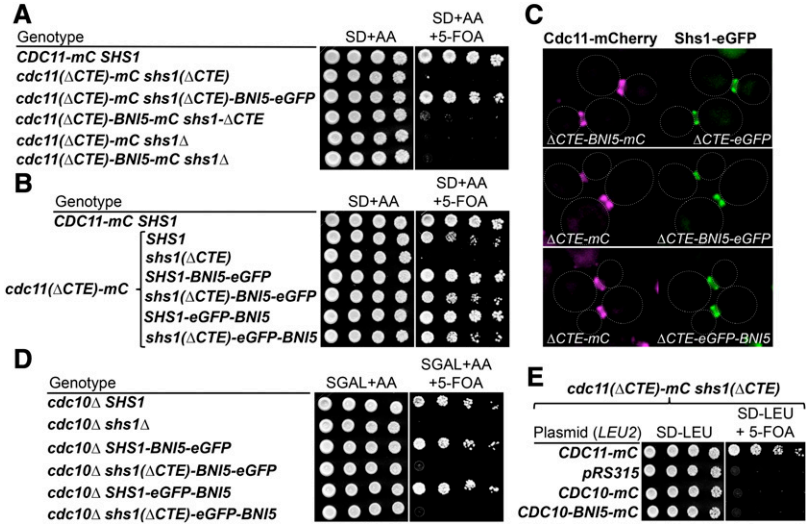

Figure 4 Fusion to Bni5 rescues the growth defect of CTE-less Shs1. (A) Strains of the indicated genotype (GFY-160, GFY-162, GFY-573, GFY-646, GFY-166, and GFY-579) were tested for their ability to grow after spotting onto control medium or the same medium containing 5-FOA to select against the covering *URA3*-marked *CDC11*-expressing plasmid. (B) Strains of the indicated genotype (GFY-160, GFY-157, GFY-162, GFY-911, GFY-913, GFY-888, and GFY-890) were tested for their ability to grow, as in A. (C) Exponentially growing cultures of cells coexpressing *cdc11(ΔCTE)-BNI5-mC* and *shs1(ΔCTE)-eGFP* (GFY-646), or *cdc11(ΔCTE)-mC* and *shs1(ΔCTE)-BNI5-eGFP* (GFY-913), or *cdc11(ΔCTE)-mC* and *shs1(ΔCTE)-eGFP-BNI5* (GFY-890), as indicated, were examined by fluorescence microscopy. White dotted line, cell periphery. (D) Strains of the indicated genotype (GFY-87, GFY-137, GFY-899, GFY-901, GFY-903, and GFY-905) were tested for their ability to grow after spotting onto control medium or the same medium containing 5-FOA to select against the covering *URA3*-marked *CDC10*-expressing plasmid. (E) Cells of the *cdc11(ΔCTE)-mC shs1(ΔCTE)-eGFP* genotype (GFY-162) were transformed with *LEU2*-marked plasmids expressing either *CDC11-mC* (pGF-lVL1), nothing (pRS315), *CDC10-mC* (pGF-prelVL6), or *CDC10-BNI5-mC* (pGF-lVL255), were tested for their ability to grow after spotting onto control medium or the same medium containing 5-FOA to select against the covering *URA3*-marked *CDC11*-expressing plasmid.

incorporated at the bud neck (Figure 4C) and their expression was not toxic to the cells (data not shown). Combined with our observation that Bni5 fused to full-length Shs1 supported more robust growth of *cdc11(ΔCTE) shs1(ΔCTE)* cells than did Bni5 fusion to Shs1(ΔCTE), we suspected that some spatial restriction in the degrees of freedom available to Bni5 might be influencing its function.

Therefore, as an independent method of tethering Bni5 to the terminal septin subunits in place of their normal CTEs, we fused a small, high-affinity, anti-GFP, single-chain camelid antibody ("nanobody," NB) (Rothbauer *et al.* 2006; Kubala *et al.* 2010) to the C terminus of either CTE-less Shs1 or CTE-less Cdc11. We then assessed whether expression of only GFP-tagged Bni5 was capable of restoring growth to such *cdc11(ΔCTE) shs1(ΔCTE)-NB* or *cdc11(CTE)-NB shs1Δ* cells. When no nanobody was present on either terminal subunit, expression of neither GFP alone (from the *CDC11* promoter) nor Bni5-GFP (from the *SHS1*, *CDC11*, or native *BNI5* promoter) nor $(HA)_3$-Bni5 (from native *BNI5* promoter) was able to rescue the viability of *cdc11(ΔCTE) shs1(ΔCTE)* cells (Figure 5A, top left). Strikingly, however, in *cdc11(ΔCTE) shs1(ΔCTE)-NB* cells, expression of Bni5-GFP (from the *SHS1*, *CDC11*, or native *BNI5* promoter) supported growth of the cells, whereas neither GFP alone nor $(HA)_3$-Bni5 (Figure 5A, top right) nor Bni5 alone (Figure S5A) was able to do so. Similarly, unlike in the absence of a nanobody fusion (Figure 5A, bottom left), in *cdc11(ΔCTE)-NB shs1Δ* cells, expression of Bni5-GFP (from the *SHS1*, *CDC11*, or native *BNI5* promoter) supported growth of the cells, whereas neither GFP alone nor $(HA)_3$-Bni5 did (Figure 5A, bottom right). Conversely, when the nanobody was fused to Cdc10, expression of Bni5-GFP was unable to restore viability to either *cdc11(ΔCTE) shs1(ΔCTE)* cells or *cdc11(ΔCTE) shs1Δ* (Figure S5B). Thus, only when either Shs1 or Cdc11 was fused to the anti-GFP nanobody, and only when GFP-tagged Bni5 was also present, was suppression of the CTE-dependent growth defect observed.

Taken together, our findings demonstrate that enhancing the amount of Bni5 in the vicinity of the terminal septin subunits Cdc11 and Shs1—whether by overexpression, by direct protein fusion, or by indirect nanobody-mediated tethering—is sufficient to bypass the requirement for the essential function of their CTE domains.

It has been reported that Bni5 participates in recruiting the type II myosin heavy chain Myo1 to the bud neck at the early stages of actomyosin ring formation (Fang *et al.* 2010). Hence, following the same logic as for Bni5 itself, we tested whether direct nanobody-mediated targeting of Myo1-GFP itself would also be sufficient to provide detectable restoration of growth to cells in which Cdc11 and Shs1 lack their CTEs. Indeed, expression of Myo1-GFP was able to rescue the growth of both *cdc11(ΔCTE) shs1(ΔCTE)-NB* cells (Figure 5B, upper panels) and *cdc11(ΔCTE)-NB shs1Δ* cells (Figure 5B, lower panels), although less robustly than Bni5 itself. Importantly, this effect was specific to Myo1-GFP because neither GFP alone or GFP-tagged versions of two other bud neck-associated proteins (Nis1 and Syp1) were unable to support any detectable growth. These results support the conclusion that a major role for CTE-mediated recruitment of Bni5 by Cdc11 and Shs1 is to assist in localizing a pool of Myo1 molecules at these positions within the septin collar at the bud neck.

Shs1 CTE is necessary and sufficient for optimal Bni5 recruitment and subsequent Myo1 localization at the bud neck

To confirm these conclusions, we examined, first, localization of GFP-Bni5 expressed at its endogenous level in WT

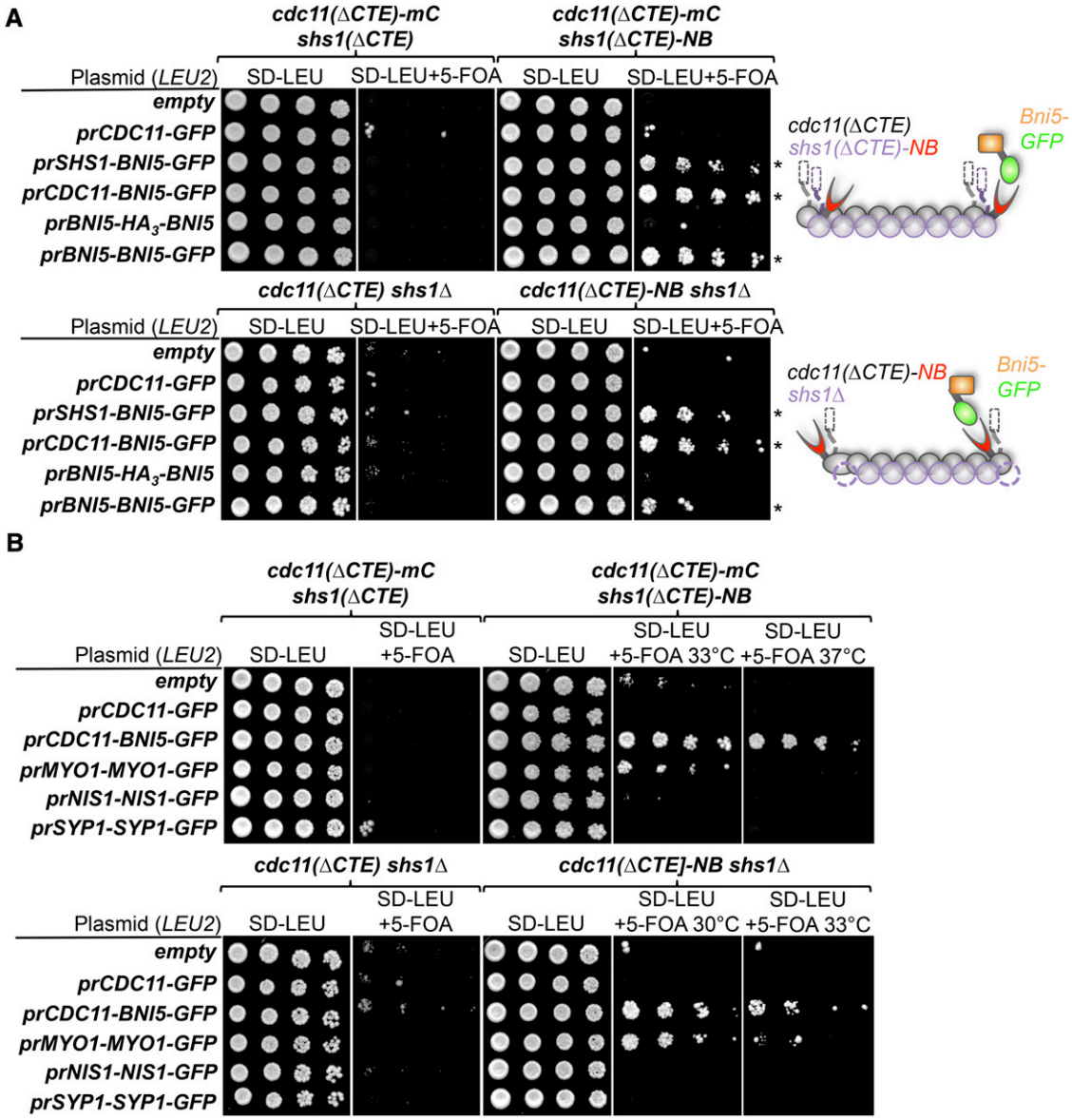

Figure 5 Tethering of Bni5-GFP or Myo1-GFP via nanobody binding rescues the growth defect of CTE-less Shs1 and Cdc11. (A, upper panel) A *cdc11(ΔCTE)-mC shs1(ΔCTE)* strain (GFY-861) and an otherwise identical strain (GFY-1295) in which a high-affinity, 117-residue, anti-GFP, camelid-derived single-chain antibody ("nanobody," NB) (Rothbauer *et al.* 2006; Kubala *et al.* 2010) was fused in-frame at the C terminus of *shs1(ΔCTE)* locus, as indicated schematically to the right, were transformed with an empty *LEU2*-marked *CEN* vector (pRS315), or the same vector expressing free GFP from the *CDC11* promoter (pGF-IVL216) or Bni5-GFP from the *SHS1* promoter (pGF-IVL384), the *CDC11* promoter (pGF-IVL385), or the *BNI5* promoter (pGF-IVL585), or N-terminally 3XHA-tagged Bni5 from the *BNI5* promoter (pGF-IVL473), were propagated overnight at 30° on SD −Ura −Leu to maintain selection for the *LEU2*-marked vectors as well as for the covering *URA3*-marked *CDC11*-expressing plasmid, then spotted onto SD −Leu medium without or with 5-FOA to remove the covering plasmid, and incubated at 37° for 3 days. (Lower panel) A *cdc11(ΔCTE) shs1Δ* strain (GFY-851) and an otherwise identical strain (GFY-1291) in which the NB was fused in-frame to the C terminus of the *cdc11(ΔCTE)* locus, as indicated schematically to the right, were transformed with the same set of *LEU2*-marked plasmids, propagated on SD −Ura −Leu, then spotted onto SD −Leu medium without or with 5-FOA to remove the covering *URA3*-marked *CDC11*-expressing plasmid, and incubated at 30° for 3 days. Gray spheres, Cdc11-capped heterooctamers; purple spheres, Shs1-capped heterooctamers; dotted cylinders and broken line, CTE deletions; dotted circles, deletion of Shs1; red semicircle, anti-GFP nanobody; Bni5 (orange)-GFP (green) fusion protein. (B) The same pairs of strains as in A were transformed with an empty *LEU2*-marked *CEN* vector (pRS315), or the same vector expressing either free GFP (pGF-IVL216) or Bni5-GFP (pGF-IVL385) from the *CDC11* promoter, or Myo1-GFP (pGF-IVL425), Nis1-GFP (pGF-IVL553), or Syp1-GFP (pGF-IVL559) from their native promoters, and then propagated and tested for growth in the absence of the covering *URA3*-marked *CDC11*-expressing plasmid as in A at two different temperatures, either 33° and 37° (upper panel) or 30° and 33° (lower panel), as indicated.

cells and in otherwise isogenic derivatives in which we removed or otherwise manipulated the CTEs of Shs1 and Cdc11 and in which we marked the septin collar at the bud neck with Cdc10-mCherry. N-terminally tagged Bni5 complements *bni5Δ* cells almost as well as untagged Bni5 (Figure S3A) and localizes efficiently to the septin collar at

the bud neck (Figure S3B). In cells lacking the CTE of Shs1, but retaining Cdc11 and its CTE, the level of Bni5 present at the bud neck was reduced by ~50% and the level of GFP-Bni5 in the cytosol was concomitantly increased (Figure 6A, left, compare uppermost panel to the second panel from the top; quantified in Figure 6B). In cells lacking Shs1 altogether, but retaining Cdc11 and its CTE, there was a complete loss of GFP-Bin5 at the bud neck (Figure 6A, left, compare uppermost panel to third panel from the top). Thus, for the CTE of Cdc11 to function properly with respect to association with Bni5, the Shs1 subunit must be present. Indeed, restoration of Shs1 expression in the *CDC11 shs1Δ* cells (and in the two mutant strains examined) restored a wild-type level of GFP-Bni5 at the septin collar (Figure 6A, right). Strikingly, when the CTE of Shs1 was replaced with the CTE of Cdc11 in cells already containing Cdc11 and its CTE, the level of GFP-Bni5 was again only ~50% of that observed in wild-type cells (Figure 6A, left, compare uppermost panel to bottom panel; Figure 6B), indicating that the native CTE of Shs1 is more efficacious than the CTE of Cdc11 in recruiting Bni5 to the septin collar at the bud neck.

We attempted to conduct parallel microscopy experiments to assess the role of the Cdc11 CTE in GFP-Bni5 recruitment in cells retaining Shs1 and its CTE, or lacking Shs1 and/or its CTE; however, removal of the CTE of Cdc11 in the background where both Cdc10 and Bni5 were tagged caused cells to be inviable (Figure 6C). Nevertheless, presence of either the CTE of Shs1 or the CTE of Cdc11 is all that is necessary to allow the growth of cells expressing GFP-Bni5 at its endogenous level (Figure S6A). Thus, to examine the contributions of the CTE of Cdc11, we compared the behavior of *SHS1 CDC11-mC*, *SHS1 cdc11(ΔCTE)-mC*, and *SHS1 cdc11(CTE)-CTE^{Shs1}-mC* cells. First, as judged by spot test, cells with no Cdc11 CTE, but two copies of the Shs1 CTE (*SHS1 cdc11(CTE)-CTE^{Shs1}-mC*) grew as well as the wild-type control (*SHS1 CDC11-mC*) and distinctly better than cells with no Cdc11 CTE and only one copy of the Shs1 CTE (*SHS1 cdc11(ΔCTE)-mC*) (Figure S6A). Likewise, as judged by cell morphology, cells with no Cdc11 CTE, but two copies of the Shs1 CTE (*SHS1 cdc11(CTE)-CTE^{Shs1}-mC*) more closely resembled the wild-type control (*SHS1 CDC11-mC*) (Figure S6B) and were detectably less elongated than the cells with no Cdc11 CTE and only one copy of the Shs1 CTE (*SHS1 cdc11(ΔCTE)-mC*) (Figure S6C). With regard to recruitment of GFP-Bni5 in these same three strains, we noted that presence of Shs1 and its CTE was sufficient to confer a near wild-type level of recruitment to the bud neck (Figure S6, D and E).

To determine whether the observed effects of the loss of the Shs1 and Cdc11 CTEs on the efficiency of Bni5 recruitment to the bud neck were reflected in corresponding effects on Myo1 localization, we examined the same set of strains as in Figure 6A in which Myo1-GFP was integrated and expressed from its native locus on chromosome VIII. Reassuringly, we found that the observed level of Myo1-GFP recruiment to the bud neck mirrored that of GFP-Bni5. First, even in cells that retain Cdc11 and its CTE, absence of the CTE of Shs1 reproducibly and significantly reduced the fraction of cells with a detectable Myo1-GFP signal at the septin collar (Figure 7A, compare uppermost panel to the second panel from the top; quantified in Figure 7B) and concomitantly reduced the intensity of any observed Myo1-GFP signal present at the bud neck (Figure 7C). In cells retaining Cdc11 and its CTE, but lacking Shs1 altogether, there was a dramatic decrease in the fraction of cells with a detectable Myo1-GFP signal at the bud neck (Figure 7A, compare uppermost panel to the third panel from the top), and this reduction was quite comparable to that caused by the absence of Bni5 (Figure 7B). Finally, when the CTE of Shs1 was replaced with the CTE of Cdc11 in cells already containing Cdc11 and its CTE, there was no significant increase either in the fraction of cells displaying a Myo1-GFP signal at the bud neck; Figure 7B) or in the intensity of that Myo1-GFP signal (Figure 7A, compare uppermost panel to bottom; Figure 7C). Thus, as with Bni5, the CTE of Shs1 seems to have a more predominant role in Myo1 localization than does the CTE of Cdc11.

Discussion

New mechanistic insight Into the physiological role of septin subunits Shs1 and Cdc11

The detailed genetic analysis of Shs1 and Cdc11 described in the accompanying article (Finnigan *et al.* 2015) demonstrated that, once recruited to the ends of either Cdc11-Cdc12-Cdc3-Cdc10-Cdc10-Cdc3-Cdc12-Cdc11 or Shs1-Cdc12-Cdc3-Cdc10-Cdc10-Cdc3-Cdc12-Shs1 heterooctameric rods, the element most critical for the function of each of these two terminal septin subunits is the sequence in their CTE with CC-forming propensity. For example, the CTE is necessary for Shs1 function in four different genetic backgrounds in which Shs1 is required for growth, and the CC sequence itself is sufficient because the remainder of the CTE is totally dispensable for Shs1 function. Moreover, a Cdc11(ΔCTE)-CTE^{Shs1} chimera restores viability to *cdc11(ΔCTE) shs1(ΔCTE)* cells.

Of course, the CC elements in the CTEs of Shs1 and Cdc11 could have multiple roles, such as providing cross-bracing between polymerized septin filaments (Bertin *et al.* 2010), forming networks important for three-dimensional organization of septin superstructures (Bertin *et al.* 2012; Ong *et al.* 2014), and/or driving conformational changes that direct geometric transitions in the supramolecular architecture of septin-based structures (Vrabioiu and Mitchison 2006; Meseroll *et al.* 2013). However, there were already strong hints in the literature and from our own prior work that the roles of these terminal subunits, and Shs1 in particular, were likely not in assembly of septin-derived structure *per se*, but rather in recruiting to the bud neck a factor (or factors) necessary to execute other important cellular processes. In this regard, we found that, under the

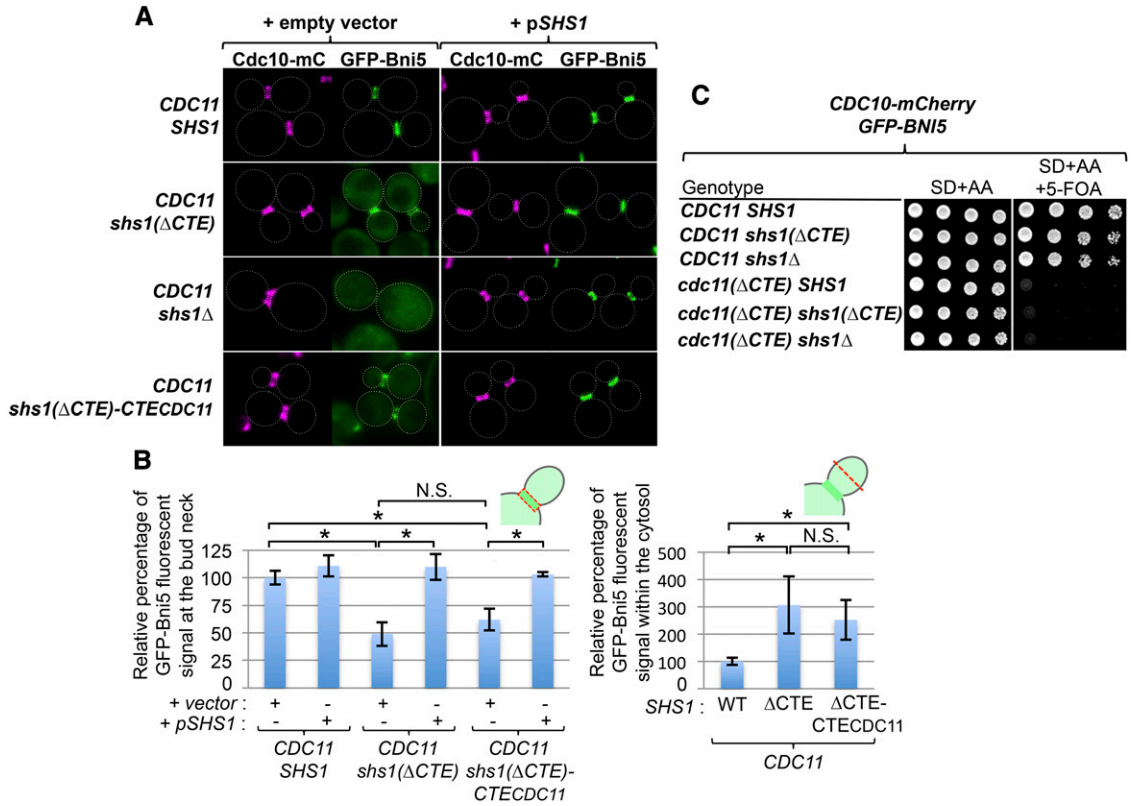

Figure 6 Recruitment of GFP-Bni5 to the bud neck is dependent on Shs1 and its CTE. (A) Samples of exponentially growing cultures of strains GFY-1316, GFY-1318, GFY-1319, and GFY-1360, each expressing both Cdc10-mC and GFP-Bni5 from their endogenous loci on, respectively, chromosomes III and XIV, and transformed with either an empty vector (pRS315) or the same vector expressing *SHS1* (pGF-V68), were visualized by fluorescence microscopy. White dotted lines, cell periphery. (B) Fluorescence intensity of the GFP-Bni5 signal in a total of 100–150 cells from each of three representative images of the indicated strains from A was measured at the bud neck (left bar graph) or in the cytosol (right bar graph) using ImageJ, as described in detail in *Materials and Methods*. Absolute values were normalized to that in the control (*CDC11 SHS1*) cells and are presented as a relative percentage (error bars are standard deviation of the mean). Because GFP-Bni5 dissociates from the bud neck upon execution of cytokinesis (see Figure S3B), only large-budded cells prior to the onset of cytokinesis, as judged by an intact septin collar and lack of formation of split rings (assessed by the Cdc10-mC pattern) were scored. Because the *shs1Δ* cells showed no GFP-Bni5 signal at the bud neck, they were not plotted. The statistical significance of the differences observed was assessed using an unpaired *t*-test. Asterisk, $P < 0.05$; N.S., not statistically significant. (C) GFY-1318, GFY-1319, and GFY-1360, and derivatives in which the *CDC11* locus was replaced with the *cdc11(ΔCTE)* allele (GFY-1315, GFY-1317, and GFY-1320, respectively), were tested for their ability to grow in the absence and presence of 5-FOA to select for loss of the covering *URA3*-marked *CDC11*-expressing plasmid.

right conditions, and when Shs1 is present, *cdc10Δ* cells can survive (McMurray *et al.* 2011; Finnigan *et al.* 2015). Viability of Cdc10-deficient cells depends on formation of nonnative Cdc11-Cdc12-Cdc3-Cdc3-Cdc12-Cdc11 heterohexamers and their end-on-end polymerization into filaments via otherwise normal Cdc11-Cdc11 interaction (McMurray *et al.* 2011). However, we (McMurray *et al.* 2011; Finnigan *et al.* 2015) and others (Iwase *et al.* 2007) have found that such *cdc10Δ* cells are inviable when Shs1 is absent. Thus, presumably, Shs1-Cdc12-Cdc3-Cdc3-Cdc12-Shs1 heterohexamers also form and contribute to optimal septin function. Because Cdc11-Cdc12-Cdc3-Cdc3-Cdc12-Cdc11 rods can polymerize into filaments regardless of the presence or absence of Shs1, it seems unlikely that lack of filament assembly *per se* explains why Shs1 is required in this sensitized background. Indeed, it had been noted that, in *shs1Δ* cells, two components of the actomyosin contractile ring (Myo1 and Iqg1) and a bud neck-localized factor necessary for chitinaceous septum formation (Cyk3) were either delocalized or mislocalized (Iwase *et al.* 2007). However, in agreement with our findings about the essential role of its CC element for Shs1 function, it was also reported that a short C-terminal truncation, Shs1(Δ519–551), which leaves the CC element in Shs1 completely intact, did not display mis- or delocalization of those factors or any cytokinesis defects (Iwase *et al.* 2007). Conversely, unlike loss of Shs1, absence of Cdc10 does not preclude localization of Myo1-GFP to the bud neck (Iwase *et al.* 2007; McMurray *et al.* 2011). If, however, Shs1 becomes essential for Myo1 neck localization when Cdc10 is absent, and Myo1 action is needed for such cells to divide, then inviability of *cdc10Δ shs1Δ* double cells likely reflects crippling of cytokinesis rather than an effect on septin filament assembly *per se*. Indeed, unlike *CDC10*$^+$ cells, a *cdc10Δ* mutant cannot grow when the level of Myo1 expression is greatly reduced (McMurray *et al.* 2011).

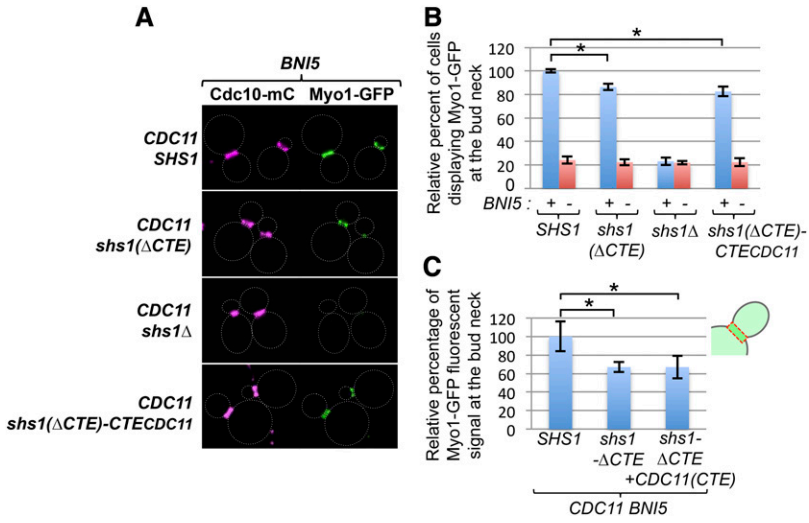

Figure 7 Myo1 recruitment to the bud neck is dependent on Bni5 and Shs1 and its CTE. (A) Samples of exponentially growing cultures of four *BNI5*$^+$ strains (GFY-1452, GFY-1453, GFY-1454, and GFY-1456), each expressing both Cdc10-mC and Myo1-GFP from their endogenous loci on, respectively, chromosomes III and VIII, were visualized by fluorescence microscopy. White dotted lines, cell periphery. (B) A total of 50–100 cells in triplicate representative images of the same strains as in A, and corresponding *bni5Δ* strains (GFY-1455, GFY-1457, GFY-1458, and GFY-1459), were examined. The percentage of the population that displayed Myo1-GFP at the bud neck was plotted relative to that exhibited by the control (*CDC11 SHS1*) cells, which was set at 100%. Statistical significance of the differences observed was assessed using an unpaired *t*-test. Asterisk, $P < 0.05$; N.S., not statistically significant. (C) Fluorescence intensity of the Myo1-GFP signal in a total of 100–150 cells from each of three representative images of the indicated strains from A was measured at the bud neck using ImageJ as in Figure 6B (left) and normalized to the value in the control (CDC11 SHS1 cells), which was set at 100% (error bars are the standard deviation of the mean). Because the *shs1Δ* cells showed no Myo1-GFP signal at the bud neck, they were not plotted.

The CC elements in the CTEs of Shs1 and Cdc11 recruit Bni5

Of the group of proteins suggested to interact (either directly or indirectly) with septins at the division site, previous evidence made Bni5 a strong candidate for the factor that associates with the CTEs of Shs1 and Cdc11. Although *BNI5* was isolated as a dosage suppressor of the temperature-sensitivity lethality of *cdc12-6*^{ts} cells, it also suppressed the growth defects of *cdc10-1*^{ts}, *cdc11-6*^{ts}, and, quite tellingly *shs1Δ* (called *sep7Δ*, at the time) cells (Lee *et al.* 2002, #62), in agreement with its ability to associate with the CTE of Cdc11. Conversely, loss of Bni5 results in an increase in formation of chains of interconnected cells, indicative of an impairment of cytokinesis, and, most revealingly, a *bni5Δ* mutation greatly exacerbated the cytokinesis defects of *cdc3-6*^{ts}, *cdc10-1*^{ts}, *cdc11-6*^{ts}, *cdc12-6*^{ts}, or, especially, *sep7Δ* cells (Lee *et al.* 2002). Bni5 localizes to the mother-bud neck in a septin-dependent manner, and its association was originally attributed, largely on the basis of two-hybrid analysis, to an interaction with the N-terminal domain of Cdc11 (Shs1/Sep7 was not tested) (Lee *et al.* 2002). However, the globular N-terminal GTP-binding domain of every septin is necessary for its proper folding, stability, and incorporation into any septin-containing complex and into the septin collar at the bud neck (Johnson *et al.* 2015). So, the two-hybrid method can be misleading when applied to the analysis of septins and their interactions, as we have pointed out previously (McMurray and Thorner 2008). Hence, our observations provide deeper mechanistic insight to explain the preceding findings. As we showed here, the essential functions of the CTEs of Shs1 and Cdc11 are bypassed by enhancing the amount of Bni5 associated with these subunits either by high-level overexpression or, at endogenous levels of expression, by direct protein fusion or by indirect nanobody-mediated tethering. Neither fusion nor nanobody tethering to Cdc10 was able to do so, demonstrating the specificity for Bni5 localization to Shs1 and Cdc11. Conversely, absence of the CTEs of Shs1 or Cdc11 clearly diminishes the amount of Bni5 found at the bud neck.

Only the C-terminal third of Bni5 is required for its function

This work also represents the first *in vivo* genetic dissection of Bni5 itself. For our analysis, we used two independent methods to assess the functionality of a set of nested N- and C-terminal truncations—their ability upon overexpression to suppress the growth defect of CTE-less Shs1 and Cdc11 cells, and their ability at an endogenous level of expression to complement the inviability of *bni5Δ* cells in a sensitized background. Both approaches yielded the identical conclusion that the C-terminalmost ~100–150 residues of this 448-residue protein are necessary and sufficient for its physiological function. Because it has been reported that phosphorylation at four Ser and Thr residues near the C terminus of Bni5 are required both for normal bud morphogenesis (Nam *et al.* 2007a) and for its association with septins and cytokinesis (Nam *et al.* 2007b), we used the same two assays to assess the veracity of these prior claims. Contrary to these previous reports, we found that neither nonphosphorylatable (Ala) alleles nor phosphomimetic (Asp) alleles, even at all four sites, displayed any significant decrement in biological function in either of our growth assays.

We found that, when greatly overexpressed, a Bni5-GFP fusion was capable of suppressing the growth phenotypes of *cdc12-6*^{ts} and CTE-less Shs1 and Cdc11 cells; however, when

expressed at its endogenous level, Bni5-GFP did not complement a *bni5Δ* mutation, in keeping with our finding that the C-terminal end of Bni5 is critical for its cellular function. Indeed, when we tagged Bni5 at its N terminus (with either fluorescent protein or epitope tags), we did not observe any significant perturbation of its function under any and all conditions that we tested. Consistent with the importance of its C-terminal end, alignment of Bni5 orthologs from the fungal clade show that the C-terminalmost ~90 residues are the most highly conserved portion of this protein. In this same regard, we have observed (G.C. Finnigan and J. Thorner, unpublished results) that both GFP-Bni5 and Bni5-GFP localize exclusively to the bud neck. Thus, efficient subcellular recruitment to the septin collar alone is not sufficient for Bni5 function. It is important to point out that all previous studies to localize Bni5 used C-terminally tagged derivatives (Lee *et al.* 2002; Nam *et al.* 2007a; Fang *et al.* 2010; Renz *et al.* 2013; Schneider *et al.* 2013).

Similar to one of the strategies we employed, one previous study examined the effect of fusing Bni5-mCherry to the C terminus of *full-length* Shs1 (Schneider *et al.* 2013). Based on microscopy alone (not growth or viability assays), this permanent tethering of C-terminally tagged Bni5 to intact Shs1 had only a minor deleterious effect on the timing of the execution of cytokinesis. The fact that, in our hands, both an Shs1-Bni5-eGFP and an Shs1-eGFP-Bni5 chimera supported robust growth, even in *cdc10Δ* cells where the rate of proliferation is already markedly slower than in wild-type cells, indicates that the detriment to maintaining (additional) Bni5 at the bud neck during cytokinesis is rather modest, despite the fact that, normally, native Bni5 is displaced from the septin ring prior to the onset of actomyosin ring ingression (Lee *et al.* 2002; Fang *et al.* 2010; Schneider *et al.* 2013).

Some of our findings suggest that orientation, or geometric or conformational flexibility, is likely important for Bni5 function. For example, despite multiple independent constructions and confirmation of production of the desired fusion protein, Cdc11(ΔCTE)-Bni5 chimeras did not display any detectable level of suppression of the growth debility of CTE-less Shs1 and Cdc11 cells. In marked contrast, coexpression of the Cdc11(ΔCTE)-anti-GFP nanobody and Bni5-GFP fusions did yield overt suppression of the growth defect of CTE-less Shs1 and Cdc11 cells.

Many questions remain about Bni5 and the mechanisms by which it associates with the CTEs of Shs1 and Cdc11. Direct biochemical evidence for physical interaction between Bni5 and individual septins and specific septin structures obtained using a novel FRET-based assay method will be presented elsewhere (E. A. Booth and J. Thorner, unpublished results).

Septins coordinate Bni5-dependent Myo1-targeting to the division site

Subsequent characterization has established that Bni5 serves to coordinate recruitment of the type II myosin (Myo1) of the actomyosin contractile ring prior to the onset of cytokinesis (Fang *et al.* 2010; Wloka *et al.* 2011; Renz *et al.* 2013; Schneider *et al.* 2013). Thus, in contrast to the Shs1(ΔCTE)-Bni5 chimera, the Cdc11(ΔCTE)-Bni5 fusion may fail to function because of some steric constraint that prevents proper recruitment of Myo1, but is avoided or overcome in the cells in which Bni5-GFP is tethered to Cdc11(ΔCTE)-NB through the intermediary nanobody. Alternatively, translational fusion of Bni5 directly to the surface of the Cdc11 GTP-binding domain may have some other detrimental effect on the ability of this septin to recruit other factors or to associate with itself, with Shs1, or with Cdc12. In any event, consistent with a primary role for Bni5 in recruiting Myo1 to the septin collar, using our nanobody approach, recruitment of Myo1-GFP itself, instead of Bni5-GFP, using either the Shs1(ΔCTE)-NB or Cdc11(ΔCTE)-NB constructs yielded readily detectable rescue of the growth of CTE-less Shs1 and Cdc11 cells, whereas neither GFP alone nor two other septin-associated proteins (Nis1-GFP and Syp1-GFP) did. Given the large size and complex tertiary and quaternary structure of the Myo1 polypeptide, we did not attempt to construct Cdc11(ΔCTE)-Myo1 or Shs1(ΔCTE)-Myo1 fusions, nor did we attempt to rescue the growth phenotype of CTE-less Cdc11 and Shs1 cells by Myo1 overexpression because, in our hands, overexpression of Myo1 is toxic even to wild-type cells (G.C. Finnigan and J. Thorner, our unpublished observations). Nevertheless, the observed rescue by forced recruitment by either protein fusion or nanobody-mediated tethering is all the more remarkable because we would anticipate that such constructs might interfere with the kinetics with which these proteins normally interact.

Nonetheless, taken together, our data strongly support the model that the CTEs of the paralogous subunits Cdc11 and Shs1 cooperate to attract the optimum level of Bni5 to the septin collar (and that, for this function, Shs1 plays the dominant role), which, in turn, ensures recruitment of the proper amount of Myo1 for timely actomyosin ring assembly (Figure 8). Others (Fang *et al.* 2010) had suggested that loss of Bni5 restricted Myo1-GFP recruitment to only large-budded cells. In agreement with that conclusion, we found a dramatic decrease (>75%) in the proportion of cells displaying Myo1-GFP at the division site in cells lacking Bni5. Moreover, our analysis demonstrates that cells lacking Shs1 display the identical phenotype. In addition, a *bni5Δ* mutation combined with any loss-of-function *shs1* allele did not display a more severe phenotype, consistent with an important role for Shs1 in the Bni5-dependent recruitment of Myo1. Residual Myo1 present in *bni5Δ* or *shs1Δ* cells likely occurs through Myo1 interaction with the septin collar-binding scaffold protein IQGAP (Iqg1) (Fang *et al.* 2010).

Interplay between the terminal septin subunits Shs1 and Cdc11

Our detailed genetic analysis of Shs1 and Cdc11 provided evidence that heterotypic Cdc11-Shs1 junctions, presumably between Cdc11-Cdc12-Cdc3-Cdc10-Cdc10-Cdc3-Cdc12-Cdc11

and Shs1-Cdc12-Cdc3-Cdc10-Cdc10-Cdc3-Cdc12-Shs1 heterooctamers, occur *in vivo* (Finnigan *et al.* 2015). Similarly, some of our observations here suggest that efficient and coordinate recruitment of Bni5 also requires formation of heterotypic Cdc11-Shs1 junctions. For example, because the CTE of Shs1 is much longer (by ~100 residues) than the CTE of Cdc11 (Versele *et al.* 2004), its CC sequence may be constitutively exposed, whereas heterotypic Shs1-Cdc11 NC interaction may be necessary to induce a conformational change that allows the CC in the CTE of Cdc11 to become accessible for association with Bni5. This scenario could explain why loss of the CTE of Shs1 is sufficient to cause a 50% drop in the intensity of GFP-Bni5 at the bud neck, whereas a *shs1Δ* allele totally eliminates GFP-Bni5 decoration at the bud neck even when wild-type Cdc11 is present.

On the other hand, some of our observations indicate that maximal Bni5 binding to Cdc11 and Shs1 may require its association with both the CTE and the GTP-binding domain of one or both of these septins. For example, under conditions where *shs1(ΔCTE) cdc11(ΔCTE)* have been incubated for a sufficient time to deplete the cell of the Cdc11 expressed from a covering plasmid, and even though the GFP-Bni5 signal at the bud neck was indeed significantly diminished, we still observed readily detectable fluorescence there (although we cannot rule out that a minor amount of residual Cdc11 is responsible for the fluorescent signal detected). However, very high level expression of Bni5 suppressed the growth debility of *cdc11(ΔCTE) shs1(ΔCTE)* cells, also consistent with some degree of interaction with their G domains.

As will be described in greater detail elsewhere (G.C. Finnigan and J. Thorner, unpublished results), it is clear that Cdc11 and Shs1 have diverged from a common ancestor and have been retained in the fungal clade, presumably because they have somewhat diversified in function. Indeed, our data demonstrate that, while the CTEs of Shs1 and Cdc11 share in common the capacity for interaction with Bni5, their roles in doing so and in other respects are not equivalent. For example, as we have shown here, *cdc11(ΔCTE)* cells exhibit a much more dramatic phenotype (with respect to both growth and cell morphology) then do *shs1(ΔCTE)* cells. This could stem from the fact that the Cdc11 CTE is involved in the recruitment of other bud neck-associated factors (in addition to Bni5) or that the Cdc11 CTE contributes to some aspect of the supramolecular architecture septin structures in a way that the Shs1 CTE does not. In this regard, we find it noteworthy that, unlike Shs1(ΔCTE), C-terminal tagging of Cdc11(ΔCTE) with mCherry further compromised its function (Finnigan *et al.* 2015), suggesting that presence of the fluorescent marker protein hinders the ability of the G domain of Cdc11 (or of Shs1 and/or its CTE at heterotypic Cdc11-Shs1 junctions) to associate with Bni5 and/or other partners. Due to insertions (total of 41 residues) within its G domain, Shs1 is presumably a significantly larger protein (Versele *et al.* 2004) and, if so, fluorescent tags appended to Shs1(ΔCTE) would consequently

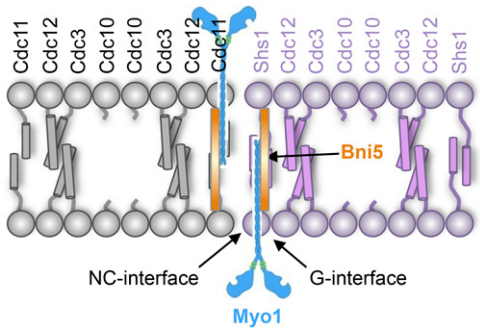

Figure 8 Schematic diagram depicting the role of the CTEs of Shs1 and Cdc11 in recruitment of Bni5 and its partner Myo1. Based on our observations that *cdc11(ΔCTE) shs1(ΔCTE)* cells are inviable, but can be rescued by high-level overexpression of Bni5, or by replacing the CTE of Shs1 with Bni5 or, by tethering Bni5-GFP or GFP-Bni5 (and even Myo1-GFP, but not by other GFP-tagged bud neck-associated proteins) to CTE-less versions of either Cdc11 or Shs1 fused to a GTP-binding nanobody, but are not rescued by similar fusions or tethering to Cdc10, indicates that a primary function of the CTE of Shs1 and an auxilliary function of the CTE of Cdc11 is to recruit Bni5 to ensure that sufficient Myo1 is localized to the bud neck for optimal timing and efficiency of actomyosin ring formation and function. Evidence presented here and in the accompanying article (Finnigan *et al.* 2015) indicates that formation of heterotypic Cdc11-Shs1 NC junctions is necessary for the proper accessibility and/or function of the CTE of Cdc11.

be located further from the core of septin complexes and filaments.

In this same regard, as presented in the accompanying article (Finnigan *et al.* 2015) and utilized here, the CTEs of Shs1 and Cdc11 are able to function in *trans* without causing a switch in septin identity. In other words, Shs1(ΔCTE)-CTE^{Cdc11} is functional, but still behaves like Shs1 (and not Cdc11); and, Cdc11(ΔCTE)-CTE^{Shs1} is functional, but still behaves like Cdc11 (and not Shs1). Thus, the distinctions between these two paralogs are largely confined to their respective G domains. In any event, the ability of these CTEs to swap chimeras to support normal growth requires Bni5. Deletion of *BNI5* in such strains caused a reproducible decrease in cell growth and a significant increase in cells with aberrant morphology. In contrast, and as expected if Bni5 executes its function when bound to these terminal subunits, we found that, for example, the growth of cells expressing the translational fusion Shs1(ΔCTE)-Bni5 was not sensitive to deletion of endogenous *BNI5*. Likewise, even though endogeneous Bni5 is present, rescue of the growth of either *cdc11(ΔCTE) shs1(ΔCTE)-NB* or *cdc11(ΔCTE)-NB shs1Δ* cells required coexpression of GFP-tagged Bni5, further confirming that Bni5 binding to the terminal subunits is critical for its function. Moreover, the morphology of dividing cells was improved when a second Shs1 CTE was added to CTE-less Cdc11, *i.e.*, in *cdc11(ΔCTE)-CTE^{Shs1} SHS1* cells.

Finally, it was reported recently that a function of Shs1, and in particular its CTE, is in formation of endoplasmic reticulum (ER)-plasma membrane junctions in order to partition this compartment between a mother and its bud (Chao *et al.* 2014). However, this conclusion was based,

first, on the effects of just two gross perturbations of Shs1 (a null allele and a complete C-terminal truncation). Second, inspection of these data shows that removal of the CTE from Shs1 had only a very modest effect (~20% reduction) on misdistribution of ER into the bud. In marked contrast, the phenotypes we have demonstrated here with regard to the CTEs of Shs1 and Cdc11, cell viability, and the recruitment of Bni5 are completely penetrant.

Acknowledgments

We thank all members of the Thorner laboratory for helpful advice and constructive suggestions during the course of this work, and Eva Nogales (University of California (UC), Berkeley), Michael McMurray (University of Colorado, Anschutz Medical Campus), and Galo Garcia (UC, San Francisco) for additional critical input. This work was supported by a Miller Research Fellowship from the Miller Institute for Basic Research in Science at UC, Berkeley (to G.C.F.) and by National Institutes of Health research grants GM21841 (to J.T.) and GM101314 (to Eva Nogales and J.T.).

Literature Cited

Alonso, A., S. D'Silva, M. Rahman, P. B. Meluh, J. Keeling *et al.*, 2012 The yeast homologue of the microtubule-associated protein Lis1 interacts with the SUMOylation machinery and a SUMO-targeted ubiquitin ligase. Mol. Biol. Cell 23: 4552–4566.

Asano, S., J. E. Park, L. R. Yu, M. Zhou, K. Sakchaisri *et al.*, 2006 Direct phosphorylation and activation of a Nim1-related kinase Gin4 by Elm1 in budding yeast. J. Biol. Chem. 281: 27090–27098.

Barral, Y., M. Parra, S. Bidlingmaier, and M. Snyder, 1999 Nim1-related kinases coordinate cell cycle progression with the organization of the peripheral cytoskeleton in yeast. Genes Dev. 13: 176–187.

Bertin, A., M. A. McMurray, P. Grob, S. S. Park, G. Garcia, 3rd *et al.*, 2008 *Saccharomyces cerevisiae* septins: supramolecular organization of heterooligomers and the mechanism of filament assembly. Proc. Natl. Acad. Sci. USA 105: 8274–8279.

Bertin, A., M. A. McMurray, L. Thai, G. Garcia, 3rd, V. Votin *et al.*, 2010 Phosphatidylinositol-4,5-bisphosphate promotes budding yeast septin filament assembly and organization. J. Mol. Biol. 404: 711–731.

Bertin, A., M. A. McMurray, J. Pierson, L. Thai, K. L. McDonald *et al.*, 2012 Three-dimensional ultrastructure of the septin filament network in *Saccharomyces cerevisiae*. Mol. Biol. Cell 23: 423–432.

Bessa, D., F. Pereira, R. Moreira, B. Johansson, and O. Queirós, 2012 Improved gap repair cloning in yeast: treatment of the gapped vector with Taq DNA polymerase avoids vector self-ligation. Yeast 29: 419–423.

Bouquin, N., Y. Barral, R. Courbeyrette, M. Blondel, M. Snyder *et al.*, 2000 Regulation of cytokinesis by the Elm1 protein kinase in *Saccharomyces cerevisiae*. J. Cell Sci. 113: 1435–1445.

Buttery, S. M., S. Yoshida, and D. Pellman, 2007 Yeast formins Bni1 and Bnr1 utilize different modes of cortical interaction during the assembly of actin cables. Mol. Biol. Cell 18: 1826–1838.

Buttery, S. M., K. Kono, E. Stokasimov, and D. Pellman, 2012 Regulation of the formin Bnr1 by septins anda MARK/Par1-family septin-associated kinase. Mol. Biol. Cell 23: 4041–4053.

Chao, J. T., A. K. Wong, S. Tavassoli, B. P. Young, A. Chruscicki *et al.*, 2014 Polarization of the endoplasmic reticulum by ER-septin tethering. Cell 158: 620–632.

Chen, H., C. C. Kuo, H. Kang, A. S. Howell, T. R. Zyla *et al.*, 2012 Cdc42p regulation of the yeast formin Bni1p mediated by the effector Gic2p. Mol. Biol. Cell 23: 3814–3826.

Claret, S., X. Gatti, F. Doignon, D. Thoraval, and M. Crouzet, 2005 The Rgd1p Rho GTPase-activating protein and the Mid2p cell wall sensor are required at low pH for protein kinase C pathway activation and cell survival in *Saccharomyces cerevisiae*. Eukaryot. Cell 4: 1375–1386.

Crutchley, J., K. M. King, M. A. Keaton, L. Szkotnicki, D. A. Orlando *et al.*, 2009 Molecular dissection of the checkpoint kinase Hsl1p. Mol. Biol. Cell 20: 1926–1936.

Dolat, L., Q. Hu, and E. T. Spiliotis, 2014 Septin functions in organ system physiology and pathology. Biol. Chem. 395: 123–141.

Edelstein, A., N. Amodaj, K. Hoover, R. Vale, and N. Stuurman, 2010 Computer control of microscopes using microManager. Curr Protoc Mol Biol Chapter 14: Unit14.20.

Estey, M. P., C. Di Ciano-Oliveira, C. D. Froese, M. T. Bejide, and W. S. Trimble, 2010 Distinct roles of septins in cytokinesis: SEPT9 mediates midbody abscission. J. Cell Biol. 191: 741–749.

Ewers, H., T. Tada, J. D. Petersen, B. Racz, M. Sheng *et al.*, 2014 A septin-dependent diffusion barrier at dendritic spine necks. PLoS One 9**:** e113916.1–e113916.19.

Fang, X., J. Luo, R. Nishihama, C. Wloka, C. Dravis *et al.*, 2010 Biphasic targeting and cleavage furrow ingression directed by the tail of a myosin II. J. Cell Biol. 191: 1333–1350.

Finnigan, G. C., J. Tagaki, C. Cho and J. Thorner, 2015 Comprehensive genetic analysis of paralogous terminal septin subunits Shs1 and Cdc11 in *Saccharomyces cerevisiae*. Genetics 200: 821–841.

Füchtbauer, A., L. B. Lassen, A. B. Jensen, J. Howard, S. Quiroga Ade *et al.*, 2011 Septin9 is involved in septin filament formation and cellular stability. Biol. Chem. 392: 769–777.

Gao, L., W. Liu, and A. Bretscher, 2010 The yeast formin Bnr1p has two localization regions that show spatially and temporally distinct association with septin structures. Mol. Biol. Cell 21: 1253–1262.

Gao, X. D., L. M. Sperber, S. A. Kane, Z. Tong, A. H. Tong *et al.*, 2007 Sequential and distinct roles of the cadherin domain-containing protein Axl2p in cell polarization in yeast cell cycle. Mol. Biol. Cell 18: 2542–2560.

Garcia, 3rd, G., A. Bertin, Z. Li, Y. Song, M. A. McMurray *et al.*, 2011 Subunit-dependent modulation of septin assembly: budding yeast septin Shs1 promotes ring and gauze formation. J. Cell Biol. 195: 993–1004.

Ghossoub, R., Q. Hu, and M. Failler, M. C. Rouyez, B. Spitzbarth *et al.*, 2013 Septins 2, 7 and 9 and MAP4 colocalize along the axoneme in the primary cilium and control ciliary length. J. Cell Sci. 126: 2583–2594.

Gilden, J. K., S. Peck, Y. C. Chen, and M. F. Krummel, 2012 The septin cytoskeleton facilitates membrane retraction during motility and blebbing. J. Cell Biol. 196: 103–114.

Gladfelter, A. S., J. R. Pringle, and D. J. Lew, 2001 The septin cortex at the yeast mother-bud neck. Curr. Opin. Microbiol. 4: 681–689.

Goldstein, A. L., and J. H. McCusker, 1999 Three new dominant drug resistance cassettes for gene disruption in *Saccharomyces cerevisiae*. Yeast 15: 1541–1553.

Gong, T., Y. Liao, F. He, Y. Yang, D. D. Yang *et al.*, 2013 Control of polarized growth by the Rho family GTPase Rho4 in budding yeast: requirement of the N-terminal extension of Rho4 and regulation by the Rho GTPase-activating protein Bem2. Eukaryot. Cell 12: 368–377.

Graziano, B. R., and E. M. Jonasson, J. G. Pullen, C. J. Gould, and B. L. Goode, 2013 Ligand-induced activation of a formin-NPF pair leads to collaborative actin nucleation. J. Cell Biol. 201: 595–611.

Hall, P. A., and S. E. Russell, 2012 Mammalian septins: dynamic heteromers with roles in cellular morphogenesis and compartmentalization. J. Pathol. 226: 287–299.

Hoang, M. L., R. P. Leon, L. Pessoa-Brandao, S. Hunt, M. K. Raghuraman *et al.*, 2007 Structural changes in Mcm5 protein bypass Cdc7-Dbf4 function and reduce replication origin efficiency in *Saccharomyces cerevisiae*. Mol. Cell. Biol. 27: 7594–7602.

Hu, Q., L. Milenkovic, H. Jin, M. P. Scott, M. V. Nachury *et al.*, 2010 A septin diffusion barrier at the base of the primary cilium maintains ciliary membrane protein distribution. Science 329: 436–439.

Huh, W. K., J. V. Falvo, L. C. Gerke, A. S. Carroll, R. W. Howson *et al.*, 2003 Global analysis of protein localization in budding yeast. Nature 425: 686–691.

Iwase, M., and A. Toh-e, 2001 Nis1 encoded by YNL078W: a new neck protein of *Saccharomyces cerevisiae*. Genes Genet. Syst. 76: 335–343.

Iwase, M., J. Luo, E. Bi, and A. Toh-e, 2007 Shs1 plays separable roles in septin organization and cytokinesis in *Saccharomyces cerevisiae*. Genetics 177: 215–229.

Johnson, C. R., A. D. Weems, J. M. Brewer, J. Thorner, and M. A. McMurray, 2015 Cytosolic chaperones mediate quality control of higher-order septin assembly in budding yeast. Mol. Biol. Cell 26: 1323–1344.

Kang, P. J., M. E. Lee, and H. O. Park, 2014 Bud3 activates Cdc42 to establish a proper growth site in budding yeast. J. Cell Biol. 206: 19–28.

Kelley, L. A., and M. J. E. Sternberg, 2009 Protein structure prediction on the Web: a case study using the Phyre server. Nat. Protoc. 4: 363–371.

Kikyo, M., K. Tanaka, T. Kamei, K. Ozaki, T. Fujiwara *et al.*, 1999 An FH domain-containing Bnr1p is a multifunctional protein interacting with a variety of cytoskeletal proteins in *Saccharomyces cerevisiae*. Oncogene 18: 7046–7054.

Kim, M. S., C. D. Froese, M. P. Estey, and W. S. Trimble, 2011 occupies the terminal positions in septin octamers and mediates polymerization-dependent functions in abscission. J. Cell Biol. 195: 815–826.

Kitada, K., A. L. Johnson, L. H. Johnston, and A. Sugino, 1993 A multicopy suppressor gene of the *Saccharomyces cerevisiae* G1 cell cycle mutant gene *dbf4* encodes a protein kinase and is identified as *CDC5*. Mol. Cell. Biol. 13: 4445–4457.

Kitazono, A. A., 2009 Improved gap-repair cloning method that uses oligonucleotides to target cognate sequences. Yeast 26: 497–505.

Knaus, M., M. P. Pelli-Gulli, F. van Drogen, S. Springer, M. Jaquenoud *et al.*, 2007 Phosphorylation of Bem2p and Bem3p may contribute to local activation of Cdc42p at bud emergence. EMBO J. 26: 4501–4513.

Kota, J., and P. O. Ljungdahl, 2005 Specialized membrane-localized chaperones prevent aggregation of polytopic proteins in the ER. J. Cell Biol. 168: 79–88.

Kozubowski, L., H. Panek, A. Rosenthal, A. Bloecher, D. J. DeMarini *et al.*, 2003 A Bni4-Glc7 phosphatase complex that recruits chitin synthase to the site of bud emergence. Mol. Biol. Cell 14: 26–39.

Kubala, M. H., O. Kovtun, K. Alexandrov, and B. M. Collins, 2010 Structural and thermodynamic analysis of the GFP: GFP-nanobody complex. Protein Sci. 19: 2389–2401.

Kumar, A., S. Agarwal, J. A. Heyman, S. Matson, M. Heidtman *et al.*, 2002 Subcellular localization of the yeast proteome. Genes Dev. 16: 707–719.

Lee, P. R., S. Song, H. S. Ro, C. J. Park, J. Lippincott *et al.*, 2002 Bni5p, a septin-interacting protein, is required for normal septin function and cytokinesis in *Saccharomyces cerevisiae*. Mol. Cell. Biol. 22: 6906–6920.

Makanae, K., R. Kintaka, T. Makino, H. Kitano, and H. Moriya, 2013 Identification of dosage-sensitive genes in *Saccharomyces cerevisiae* using the genetic tug-of-war method. Genome Res. 23: 300–311.

McMurray, M. A., and J. Thorner, 2008 Biochemical properties and supramolecular architecture of septin hetero-oligomers and septin filaments, pp. 49–100 in *The Septins*, edited by P. A. Hall, S. E. G. Russell, and J. R. Pringle. John Wiley & Sons, Chichester, West Sussex.

McMurray, M. A., A. Bertin, G. Garcia, 3rd, L. Lam, E. Nogales *et al.*, 2011 Septin filament formation is essential in budding yeast. Dev. Cell 20: 540–549.

Meitinger, F., M. E. Boehm, A. Hofmann, B. Hub, H. Zentgraf *et al.*, 2011 Phosphorylation-dependent regulation of the F-BAR protein Hof1 during cytokinesis. Genes Dev. 25: 875–888.

Meitinger, F., S. Palani, B. Hub, and G. Pereira, 2013 Dual function of the NDR-kinase Dbf2 in the regulation of the F-BAR protein Hof1 during cytokinesis. Mol. Biol. Cell 24: 1290–1304.

Meitinger, F., A. Khmelinskii, S. Morlot, S. Kurtulmus, S. Palani *et al.*, 2014 A memory system of negative polarity cues prevents replicative aging. Cell 159: 1056–1069.

Meseroll, R. A., P. Occhipinti, and A. S. Gladfelter, 2013 Septin phosphorylation and coiled-coil domains function in cell and septin ring morphology in the filamentous fungus *Ashbya gossypii*. Eukaryot. Cell 12: 182–193.

Mino, A., K. Tanaka, T. Kamei, M. Umikawa, T. Fujiwara *et al.*, 1998 Shs1p: a novel member of septin that interacts with Spa2p, involved in polarized growth in *Saccharomyces cerevisiae*. Biochem. Biophys. Res. Commun. 251: 732–736.

Moriya, H., and K. Isono, 1999 Analysis of genetic interactions between *DHH1*, *SSD1* and *ELM1* indicates their involvement in cellular morphology determination in *Saccharomyces cerevisiae*. Yeast 15: 481–496.

Mortensen, E. M., H. McDonald, J. Yates, 3rd, and D. R. Kellogg, 2002 Cell cycle-dependent assembly of a Gin4-septin complex. Mol. Biol. Cell 13: 2091–2105.

Mostowy, S., M. Bonazzi, M. A. Hamon, T. N. Tham, A. Mallet *et al.*, 2010 Entrapment of intracytosolic bacteria by septin cage-like structures. Cell Host Microbe 8: 433–444.

Muhlrad, D., R. Hunter, and R. Parker, 1992 A rapid method for localized mutagenesis of yeast genes. Yeast 8: 79–82.

Mumberg, D., R. Müller, and M. Funk, 1994 Regulatable promoters of *Saccharomyces cerevisiae*: comparison of transcriptional activity and their use for heterologous expression. Nucleic Acids Res. 22: 5767–5768.

Nam, S. C., H. Sung, Y. B. Chung, C. K. Lee, D. H. Lee *et al.*, 2007a Requirement of Bni5 phosphorylation for bud morphogenesis in *Saccharomyces cerevisiae*. J. Microbiol. 45: 34–40.

Nam, S. C., H. Sung, S. H. Kang, J. Y. Joo, S. J. Lee *et al.*, 2007b Phosphorylation-dependent septin interaction of Bni5 is important for cytokinesis. J. Microbiol. 45: 227–233.

Nishihama, R., J. H. Schreiter, M. Onishi, E. A. Vallen, J. Hanna *et al.*, 2009 Role of Inn1 and its interactions with Hof1 and Cyk3 in promoting cleavage furrow and septum formation in *S. cerevisiae*. J. Cell Biol. 185: 995–1012.

Okuzaki, D., S. Tanaka, H. Kanazawa, and H. Nojima, 1997 Gin4 of *S. cerevisiae* is a bud neck protein that interacts with the Cdc28 complex. Genes Cells 2: 753–770.

Okuzaki, D., T. Watanabe, S. Tanaka, and H. Nojima, 2003 The *Saccharomyces cerevisiae* bud-neck proteins Kcc4 and Gin4 have distinct but partially-overlapping cellular functions. Genes Genet. Syst. 78: 113–126.

Ong, K., C. Wloka, S. Okada, T. Svitkina, and E. Bi, 2014 Architecture and dynamic remodelling of the septin cytoskeleton during the cell cycle. Nat. Commun. 5: 5698.1–5698.10.

Ono, N., T. Yabe, M. Sudoh, T. Nakajima, T. Yamada-Okabe *et al.*, 2000 The yeast Chs4 protein stimulates the trypsin-sensitive activity of chitin synthase 3 through an apparent protein-protein interaction. Microbiology 146: 385–391.

Renz, C., N. Johnsson, and T. Gronemeyer, 2013 An efficient protocol for the purification and labeling of entire yeast septin rods from *E. coli* for quantitative *in vitro* experimentation. BMC Biotechnol. 13: 60.

Roelants, F. M., B. M. Su, J. von Wulffen, S. Ramachandran, E. Sartorel *et al.*, 2015 Protein kinase Gin4 negatively regulates flippase function and controls plasma membrane asymmetry. J. Cell Biol. 208: 299–311.

Roeseler, S., K. Sandrock, I. Bartsch, and B. Zieger, 2009 Septins, a novel group of GTP-binding proteins: relevance in hemostasis, neuropathology and oncogenesis. Klin. Padiatr. 221: 150–155.

Roncero, C., and Y. Sánchez, 2010 Cell separation and the maintenance of cell integrity during cytokinesis in yeast: the assembly of a septum. Yeast 27: 521–530.

Rothbauer, U., K. Zolghadr, S. Tillib, D. Nowak, L. Schermelleh *et al.*, 2006 Targeting and tracing antigens in live cells with fluorescent nanobodies. Nat. Methods 3: 887–889.

Saarikangas, J., and Y. Barral, 2011 The emerging functions of septins in metazoans. EMBO Rep. 12: 1118–1126.

Sakchaisri, K., S. Asano, L. R. Yu, M. J. Shulewitz, C. J. Park *et al.*, 2004 Coupling morphogenesis to mitotic entry. Proc. Natl. Acad. Sci. USA 101: 4124–4129.

Sambrook, J., and D. W. Russell, 2001 *Molecular Cloning: A Laboratory Manual*, Cold Spring Harbor Laboratory Press, Cold Spring Harbor, NY.

Schneider, C., J. Grois, C. Renz, T. Gronemeyer, and N. Johnsson, 2013 Septin rings act as a template for myosin higher-order structures and inhibit redundant polarity establishment. J. Cell Sci. 126: 3390–3400.

Sellin, M. E., L. Sandblad, S. Stenmark, and M. Gullberg, 2011 Deciphering the rules governing assembly order of mammalian septin complexes. Mol. Biol. Cell 22: 3152–3164.

Sellin, M. E., S. Stenmark, and M. Gullberg, 2014 Cell type-specific expression of SEPT3-homology subgroup members controls the subunit number of heteromeric septin complexes. Mol. Biol. Cell 25: 1594–1607.

Sharma, S., A. Quintana, G. M. Findlay, M. Mettlen, B. Baust *et al.*, 2013 An siRNA screen for NFAT activation identifies septins as coordinators of store-operated Ca^{2+} entry. Nature 499: 238–242.

Shulewitz, M. J., C. J. Inouye, and J. Thorner, 1999 Hsl7 localizes to a septin ring and serves as an adapter in a regulatory pathway that relieves tyrosine phosphorylation of Cdc28 protein kinase in *Saccharomyces cerevisiae*. Mol. Cell. Biol. 19: 7123–7137.

Sikorski, R. S., and P. Hieter, 1989 A system of shuttle vectors and yeast host strains designed for efficient manipulation of DNA in *Saccharomyces cerevisiae*. Genetics 122: 19–27.

Smith, G. R., S. A. Givan, P. Cullen, and G. F. J. Sprague, 2002 GTPase-activating proteins for Cdc42. Eukaryot. Cell 1: 469–480.

Sopko, R., D. Huang, N. Preston, G. Chua, B. Papp *et al.*, 2006 Mapping pathways and phenotypes by systematic gene overexpression. Mol. Cell 21: 319–330.

Stevenson, L. F., B. K. Kennedy, and E. Harlow, 2001 A large-scale overexpression screen in *Saccharomyces cerevisiae* identifies previously uncharacterized cell cycle genes. Proc. Natl. Acad. Sci. USA 98: 3946–3951.

Sugino, Y., K. Ichioka, T. Soda, M. Ihara, M. Kinoshita *et al.*, 2008 Septins as diagnostic markers for a subset of human asthenozoospermia. J. Urol. 180: 2706–2709.

Tada, T., A. Simonetta, M. Batterton, M. Kinoshita, D. Edbauer *et al.*, 2007 Role of septin cytoskeleton in spine morphogenesis and dendrite development in neurons. Curr. Biol. 17: 1752–1758.

Tian, C., Y. Wu, and N. Johnsson, 2014 Stepwise and cooperative assembly of a cytokinetic core complex in *Saccharomyces cerevisiae*. J. Cell Sci. 127: 3614–3624.

Tooley, A. J., J. Gilden, J. Jacobelli, P. Beemiller, W. S. Trimble *et al.*, 2009 Amoeboid T lymphocytes require the septin cytoskeleton for cortical integrity and persistent motility. Nat. Cell Biol. 11: 17–26.

Toure, A., B. Rode, G. R. Hunnicutt, D. Escalier, and G. Gacon, 2011 Septins at the annulus of mammalian sperm. Biol. Chem. 392: 799–803.

Trimble, W. S., and S. Grinstein, 2015 Barriers to the free diffusion of proteins and lipids in the plasma membrane. J. Cell Biol. 208: 259–271.

Tu, D., B. R. Graziano, E. Park, W. Zheng, Y. Li *et al.*, 2012 Structure of the formin-interaction domain of the actin nucleation-promoting factor Bud6. Proc. Natl. Acad. Sci. USA 109: E3424–E3433.

Tully, G. H., R. Nishihama, J. R. Pringle, and D. O. Morgan, 2009 The anaphase-promoting complex promotes actomyosin-ring disassembly during cytokinesis in yeast. Mol. Biol. Cell 20: 1201–1212.

Versele, M., and J. Thorner, 2004 Septin collar formation in budding yeast requires GTP binding and direct phosphorylation by the PAK, Cla4. J. Cell Biol. 164: 701–715.

Versele, M., B. Gullbrand, M. J. Shulewitz, V. J. Cid, S. Bahmanyar *et al.*, 2004 Protein-protein interactions governing septin heteropentamer assembly and septin filament organization in *Saccharomyces cerevisiae*. Mol. Biol. Cell 15: 4568–4583.

Volceanov, L., K. Herbst, M. Biniossek, O. Schilling, D. Haller *et al.*, 2014 Septins arrange F-actin-containing fibers on the *Chlamydia trachomatis* inclusion and are required for normal release of the inclusion by extrusion. MBio 5: e01802–14.1-e01802–14.12.

Vrabioiu, A. M., and T. J. Mitchison, 2006 Structural insights into yeast septin organization from polarized fluorescence microscopy. Nature 443: 466–469.

Wloka, C., and E. Bi, 2012 Mechanisms of cytokinesis in budding yeast. Cytoskeleton (Hoboken) 69: 710–726.

Wloka, C., R. Nishihama, M. Onishi, Y. Oh, J. Hanna *et al.*, 2011 Evidence that a septin diffusion barrier is dispensable for cytokinesis in budding yeast. Biol. Chem. 392: 813–829.

Wloka, C., and E. A. Vallen, L. Thé, X. Fang, Y. Oh *et al.*, 2013 Immobile myosin-II plays a scaffolding role during cytokinesis in budding yeast. J. Cell Biol. 200: 271–286.

Wu, H., J. Guo, Y. T. Zhou, and X. D. Gao, 2015 The anillin-related region of Bud4 is the major functional determinant for Bud4's function in septin organization during bud growth and axial bud-site selection in budding yeast. Eukaryot. Cell 14: 241–251.

Yoshikawa, K., T. Tanaka, Y. Ida, C. Furusawa, T. Hirasawa *et al.*, 2011 Comprehensive phenotypic analysis of single-gene deletion and overexpression strains of *Saccharomyces cerevisiae*. Yeast 28: 349–361.

Zheng, B., J. N. Wu, W. Schober, D. E. Lewis, and T. Vida, 1998 Isolation of yeast mutants defective for localization of vacuolar vital dyes. Proc. Natl. Acad. Sci. USA 95: 11721–11726.

Zheng, L., U. Baumann and J. L. Reymond, 2004 An efficient one-step site-directed and site-saturation mutagenesis protocol. Nucleic Acids Res. 32: e115.111–e115.115.

Communicating editor: D. J. Lew

GENETICS

Supporting Information
www.genetics.org/lookup/suppl/doi:10.1534/genetics.115.176503/-/DC1

The Carboxy-Terminal Tails of Septins Cdc11 and Shs1 Recruit Myosin-II Binding Factor Bni5 to the Bud Neck in *Saccharomyces cerevisiae*

Gregory C. Finnigan, Elizabeth A. Booth, Angela Duvalyan, Elizabeth N. Liao, and Jeremy Thorner

DOI: 10.1534/genetics.115.176503

SUPPORTING INFORMATION

for

The carboxy-terminal tails of septins Cdc11 and Shs1 recruit myosin-II binding factor Bni5 to the bud neck in *Saccharomyces cerevisiae*

Gregory C. Finnigan, Elizabeth A. Booth, Angela Duvalyan, Elizabeth N. Liao

and Jeremy Thorner*

Division of Biochemistry, Biophysics and Structural Biology,

Department of Molecular and Cell Biology,

University of California, Berkeley, CA 94720-3202 USA

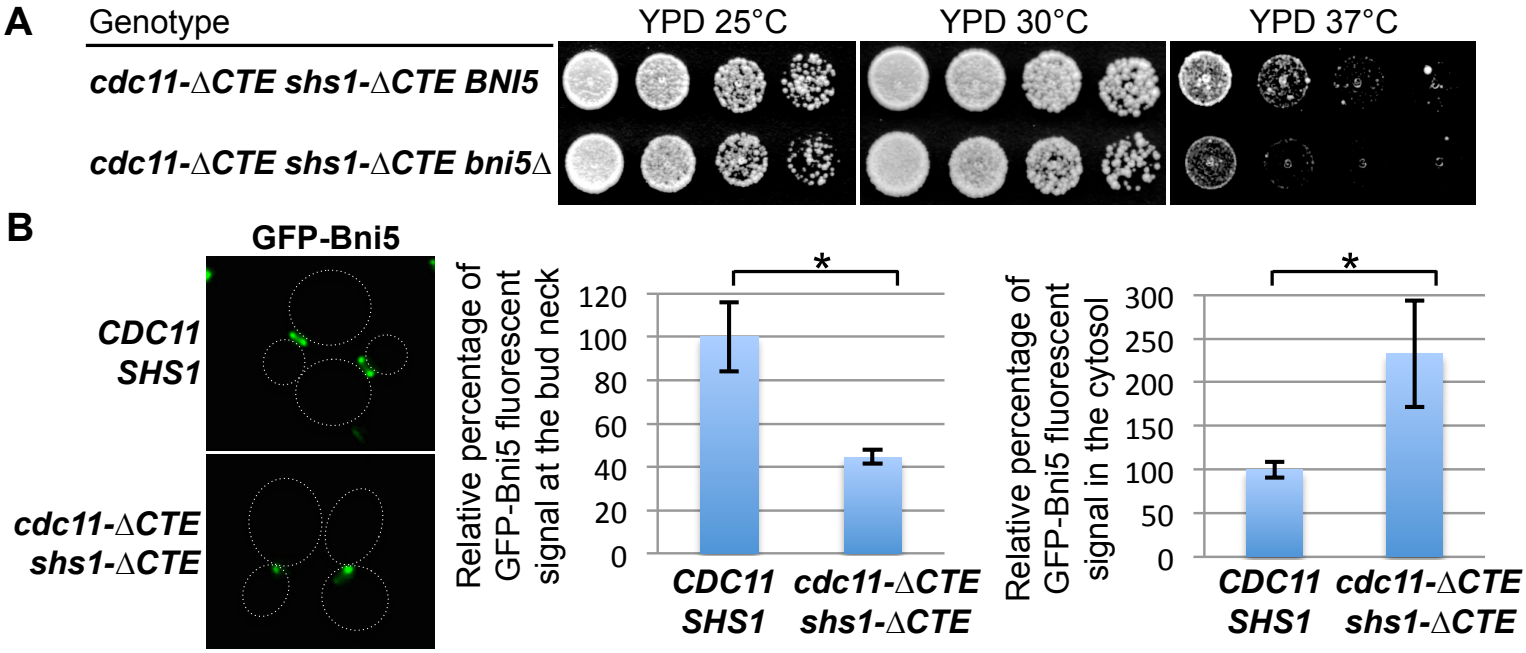

Figure S1. CTEs of Shs1 and Cdc11 play a major, but not exclusive, role in recruitment of Bni5 to the bud neck. (A) Strains GFY-870 and GFY-1113 were selected at room temperature on medium containing 5-FOA to remove the covering *URA3*-marked *CDC11*-expressing *CEN* plasmid (pJT1520), grown overnight in rich medium (YPD), spotted onto solid YPD medium, and incubated at the indicated temperature for 2 days. (B) Strains GFY-1439 and GFY-1468, each expressing GFP-Bni5 from its native promoter at its endogenous locus, were selected at room temperature on medium containing 5-FOA to remove the covering *CDC11*-expressing vector and then imaged by fluorescence microscopy (*left*). Fluorescence signal at the bud neck (*middle*) and in the cytosol (*right*) in cultures of the cells shown were quantified using ImageJ as described in Materials and Methods. Triplicate samples of (50-100 cells) for each strain were analyzed and the absolute pixel intensities were normalized to the WT control, which was set at 100%; error bar represents standard deviation of the mean. Asterisk, statistical significance ($p < 0.05$) demonstrated using an unpaired t-test.

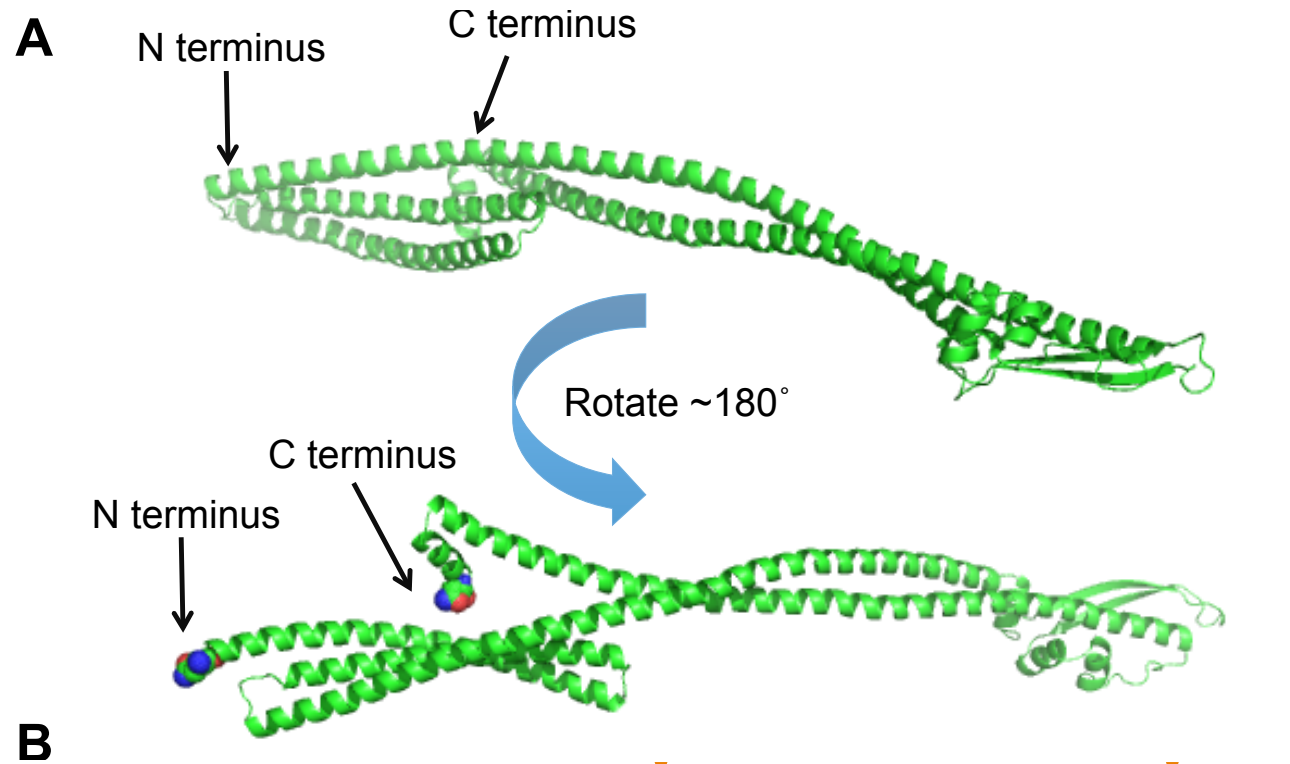

B

```
Sc_Bni5 (1)      MGLDQDKIKKRLSQIEIDINQMNQMIDENDQLVEPAEDEAVEDNVKDTGVVDAVKVAETALFSGNDGADSN----PGDSAQVEEHKTAQVHIPTENEANKSTDDPSQLS (105)
Cg_Bni5 (1)      M-LDQEDVKKRMSQIELDINQMNKMIDENDQLGENDGHDSGTEGVEG-AVGEGVDGQAGPVEPVVTTAAEE----TSETKDIEHEQVTNEGMAKE------VEDASESS (97)
Vp_Bni5 (1)      MSLDQEKIQKRLSQIEIDINQMNQMIDDNDLVNEEQQQEQQQEVEESTAEDDGGDLKNEEKTGVDESIPNE(29)VDENEDSIEVTTQEADIKEDHVEHEKEIENEQGS (134)
Kl_Bni5 (1)      M--DSEQVKKRMSQIELEISEMNEMIDKNDSIHETTVKTKQDVSSD-------------------------------------------------------------DQDEDY (50)
Zr_Bni5 (1)      MGLDKASIEKRVSRIELDIDHMNQMIDENDKLNEAGDRLEQDSRGQHAEDNQHLGSAATHQGELSREDSVQ(28)SEAVYDSQEAPVARSEASNDEYYGWSEDQQEQDE (133)
Lt_Bni5 (1)      M--DQETLRKRMSQIELEIDEMNQVIDENDQLAEPHGDEPPEHEKKKRWDSGT----------------------SKDPETGPEEPETQQVIEAELFLRSATRPVPPSI (85)
Ag_Bni5 (1)      M-MVQEKLSVKIARLEKELEALHRGVSADLRPAEDAEESESSAG-------------------------------------------------------------ERYSTDKSS (52)

Sc_Bni5 (106)    VTQPFIAKEQITHTAIAIGDSYNSFVANSAGNEKA----------------KDSCTENKEDGTVNIDQNRGE-ADVEIIENNDDE---WEDEKSDVEEGRVDKGTEENS (194)
Cg_Bni5 (98)     VQATEQAQDQQAGTNEET-NTFKTESMPEPETQAP----------------EVNDLEMKEPEMKEPEMKEPETVEPETVEPEMKE---PETVEPEMKEPVIKETDALEP (186)
Vp_Bni5 (135)    IVEAEIASETNNLKSIKEKTAMETTIEPQVLVISPNEEQKLTQRFD(38)GEVDSTEHEEPSKEEIEIEIKESIKEEIVVKEVEANTIEDEVSSPRHEEPIVKNETEEV (277)
Kl_Bni5 (51)     LELQKLTANQVDQFVQNAIKSDGEDEVPETLSSGR----------------ETALQAEEREDIKEEKP----------------GTQLEAAVVAEVVAEVQ (119)
Zr_Bni5 (134)    QAYTTGQSEADTEYDNEEEDPEETFQAPEERESQEHVNGGMQLHKR(79)PPESQSETHSETQSDIKQNEQELPTTHPYPQEIHNHQHTHETDAQELDHKEYSHETETQ (317)
Lt_Bni5 (86)     PAATELGKEQRTKPALENEPTHSEHMNQPPAERVP----------------LEQTPSDGGVSLAPSQYVDAPEAVPAQSSSKSEAAPADIGLRETQPLNGISSRQAGSVG (179)
Ag_Bni5 (53)     YASSVQAVLRARTASAASADTAMSSSTAASDSAGG----------------AKMDAADADDATRSLELR----------------LAALATQDPAVDSADTASG (124)

Sc_Bni5 (195)    E-----IESFKSPMPQNNTLGGENKLDAELVLDKFSSANKDLDIQPQT------IVVGGDNEYNHESSRLADQTPHD-----DNSENCPNRSGGSTPLDSQTKIFIPKK (287)
Cg_Bni5 (187)    E-----MKHAEIP-PQATTE--EQPTRHDEWEDVEEEEFNEIDTSTES------NNVIGDTKQVEGSSVLAAGDLRG-----NVADNG-NLTPVTDIDDAESTIFIPKK (275)
Vp_Bni5 (278)    Q-----VPEFDNEIKPGTVEEQSIDVEDLADEEILKTALEDNPIDTQIGTLESPENIESEKSTGNSMDMSNDSNIDN-----EVSDDTSSSIDTAKLEQTVLKGEIDRT (376)
Kl_Bni5 (120)    T-----EPTAEKAIPAVSVTSVPAKRIPSEKIEVSTSTEEDEAAAAAT-------IVPNTDKSSTYPAPAAIGHTQN-----GTVPRAPN--TDSSNIPTSPRILTPK- (208)
Zr_Bni5 (318)    E(23)TEQYKEVPNPPRGMEFVETREDESLDYSYEPAHQDSPETHKRTIGATQNHNSNGNSLPDTTQSVMGQGTSGEK(69)NTSQDSNGSTDNPFTSDKVYERSTSGS (510)
Lt_Bni5 (180)    S----AGSPRESQPSTETAETPSSEVDREQPDEHLQPPSEEFTTTASR-------GFKAASREDARKEMPQQSTLGNN----EPQEASAGMSFDENSPSTQSSAGSKQP (273)
Ag_Bni5 (125)    ------ASPASPAAPPSPPPSAATEGSDEAAAPLEVPKQRGDAGTAAG-------GEPVRRRPTNPFRVISVGGS-------STFKRAAGADGQASRTSSAGDKAAP-- (211)

Sc_Bni5 (288)    NSKEDGTNINHFNSDGDGQKKMANFETRRPTNPFRVISVSSNSNSRN--GSRKSSLNKYDSPV-SSPITSASELGSIAKLEKRHDYLSMKCIKLQKEIDYLNKMNAQGS (393)
Cg_Bni5 (276)    QNQ---------NSELTEQMKETLRNTRRTTNPFRVISVSSSNSSTN--SSRKSSGHDMG------LEQTPSEQ--LKRYEQRHYYLTTKCGKLQKEIDYLNKMNSQGT (365)
Vp_Bni5 (377)    ISPIEPPSQIFVAKSNMKGSVNDKQGTRRSTNPFRVVSVSGSSSPRSNPSSRHASGSSNNEPRRIPSTESTSSVNSIEKLQSRQDYLIMKCSKLQKEINYLKNMNTQGM (485)
Kl_Bni5 (209)    ----------------------------SNPFRVVHVGSQPSSRN--ASRNSSRVS--------STSSDISDINFEQLQQNYNSLSVKCTKLQKEIDYLHKFKNEST (277)
Zr_Bni5 (511)    TDTDDFIHIPKNSAQRPATTSNTPVTSRRPTNPFRVVSVGVVGPDGR--TSRKTSAGTFS-------SYKDSNVDGPAILQKKLDHLVKKCTKLQREIDYLTKMNTASS (610)
Lt_Bni5 (274)    VSPDSTQSSPQLNLPKTRNPAFPGKRATSNPNPFRVVSVTS----------------------KQTEDVSPAQKLQTRHDYLARKCIKLQREHQYLSDLRDRGA (355)
Ag_Bni5 (212)    ------------------------------------------------------------VSADEQSMLKLQRKHDYLTMKCVKLSKEIKYLPNLKKTGS (251)

Sc_Bni5 (394)    LSMEDGKRLHRAVVKLQEYLDKKTKEKYEVGVLLSRHLRKQIDRGENGQFWIGTK. (448)
Cg_Bni5 (366)    LSIDDSRKLTRAIAKLQEYLDKKNKERYEVGVLLSRQLRRDINRGENGEFWIGTK. (420)
Vp_Bni5 (486)    LSIEDSRKLNSAIQKLQDYLDRKTKEKYEVGLSLSRQLRKGVDRGENAQFWVSNK. (540)
Kl_Bni5 (278)    LTLEDRRKLITAIEKLQEYLDKKNKQRYDTGVILSRQIRKNVDMGANGQFWVGRS. (332)
Zr_Bni5 (611)    LPIEDSRKLSRAVDKLQEYLDKKNKEKYDVGVLLSRQLRREIDRGENGQFWVGTK. (665)
Lt_Bni5 (356)    VAPEDARKINSALEKLQEYLDLKTKERYEIGVLLSRQLRREIDRGENGQFWVGH.  (409)
Ag_Bni5 (252)    LSVEDTRKMNDALDKLQEYLDRKSKEKYEIGVLLSRRIRKHINNGSNGQFWLSGK. (306)
```

Figure S2. Structure prediction and sequence alignment of *S. cerevisiae* Bni5 with apparent orthologs in other fungal species. (A) Phyre[2] (KELLEY AND STERNBERG 2009) was used to model the predicted structure of *S. cerevisiae* Bni5. (B) Proteins homologous to *S. cerevisiae* Bni5 were identified using a recent version of the BLAST algorithm (NEUMANN *et al.* 2014) and aligned using CLUSTAL-W (THOMPSON *et al.* 1994). Residue numbers are given for each species: Cg, *Candida glabrata*; Vp, *Vanderwaltozyma polyspora*; Kl, *Kluyveromyces lactis*; Zr, *Zygosaccharo-myces rouxii*; Lt, *Lachancea thermotolerans*; and, Ag, *Ashbya gossypii*. Invariant residues, white letters in a black box; highly conserved residues, blue. An orange triangle marks the extent of each of the N-terminal truncations and a green triangle marks the extent of each of the C-terminal truncations generated in this study. Purple asterisks indicate Ser and Thr residues that were also analyzed.

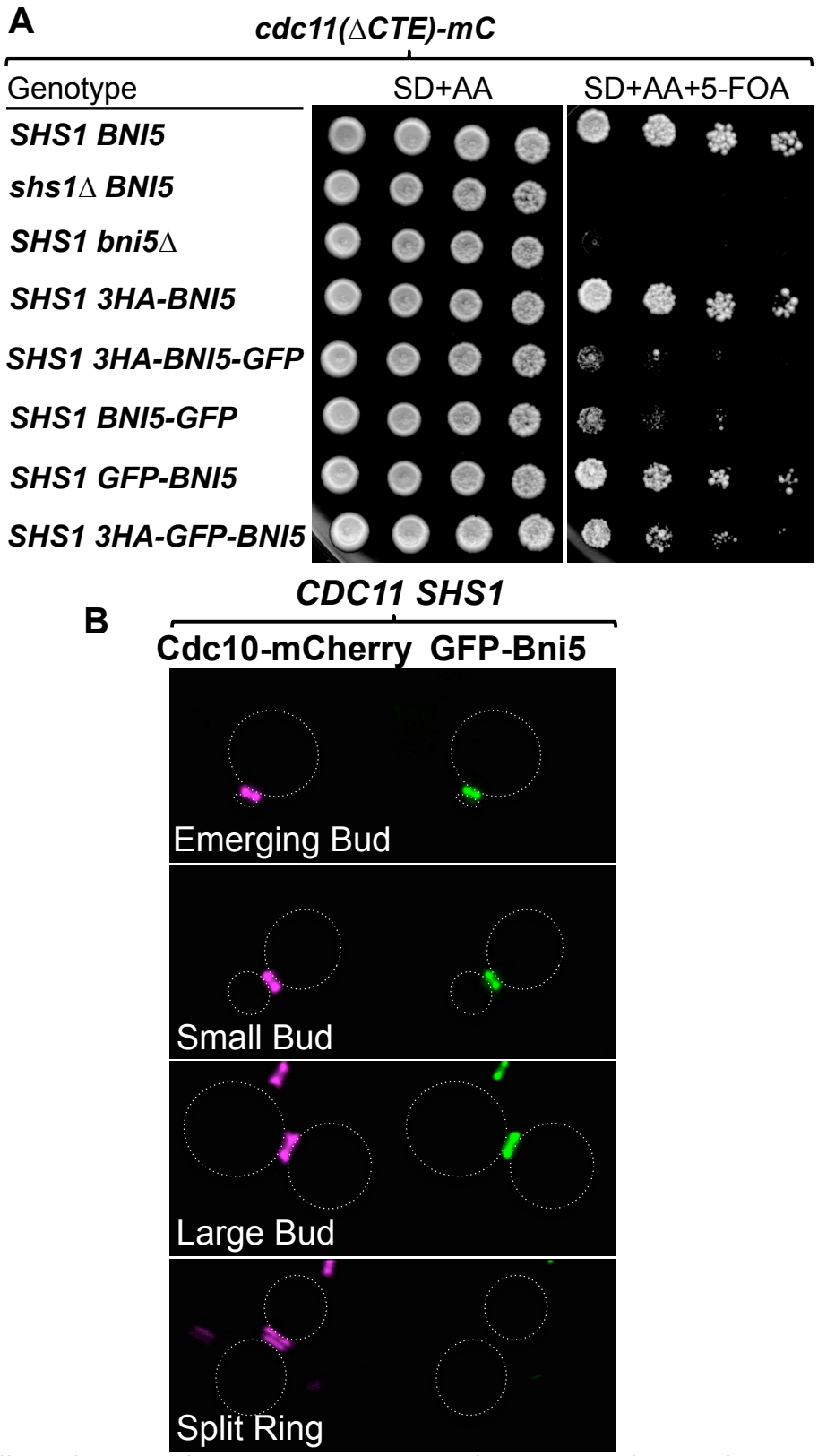

Figure S3. Effect of N- and C-terminal tags on Bni5 function. (A) Strains GFY-122, GFY-166, GFY-847, GFY-1167, GFY-1168, GFY-1236 through GFY-1238, which all contain the *cdc11-ΔCTE-mCherry* allele, which sensitizes cells to the loss of either Shs1 or Bni5, were grown overnight and spotted onto medium with or without 5-FOA to counter-select against the covering *URA3*-marked *CDC11*-expressing plasmid. (B) Strain GFY-1319 endogeously expressing both Cdc10-mCherry and GFP-Bni5 was examined by fluorescence microscopy. Representative images at the indicated stages of the cell division cycle. Cell periphery, white dotted line.

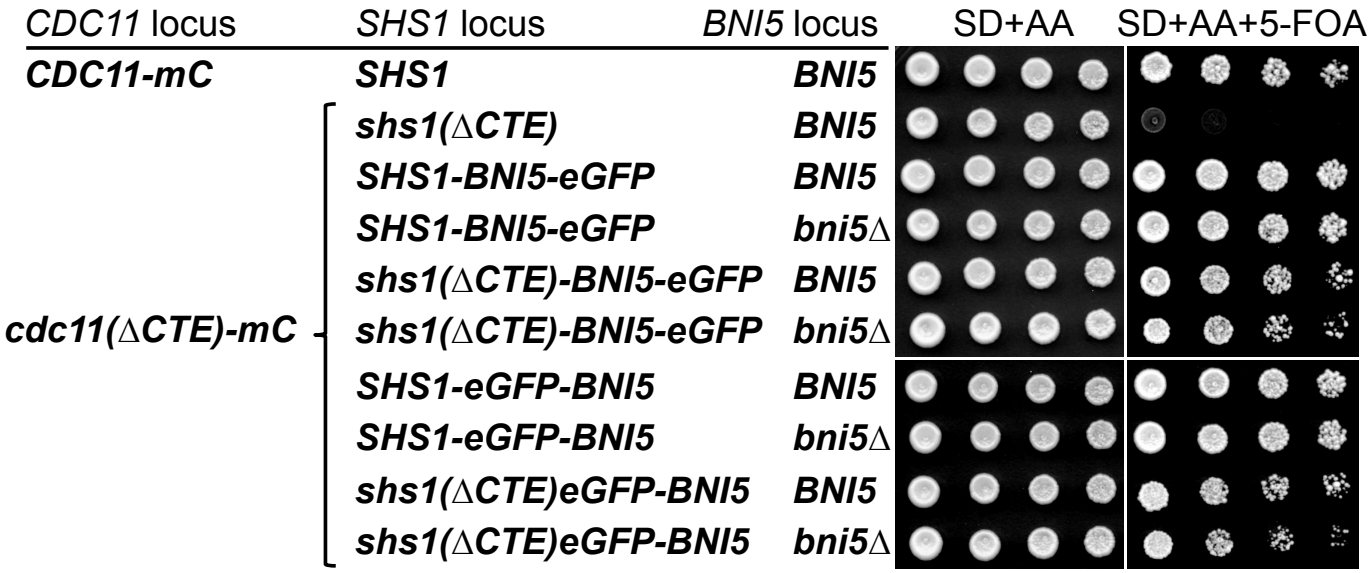

Figure S4. Endogenous Bni5 is not required for the ability of Shs1-Bni5 translational fusions to rescue growth *cdc11(ΔCTE) shs1(ΔCTE*) cells. Strains GFY-160, GFY-162, GFY-911, GFY-1104, GFY-913 and GFY-1105 were grown overnight and spotted onto medium with or without 5-FOA to select for cells that has lost the covering *URA3*-marked *CDC11*-expressing plasmid. Strains GFY-160, GFY-162, GFY-888, GFY-1102, GFY-890 and GFY-1103 were also tested in the same way.

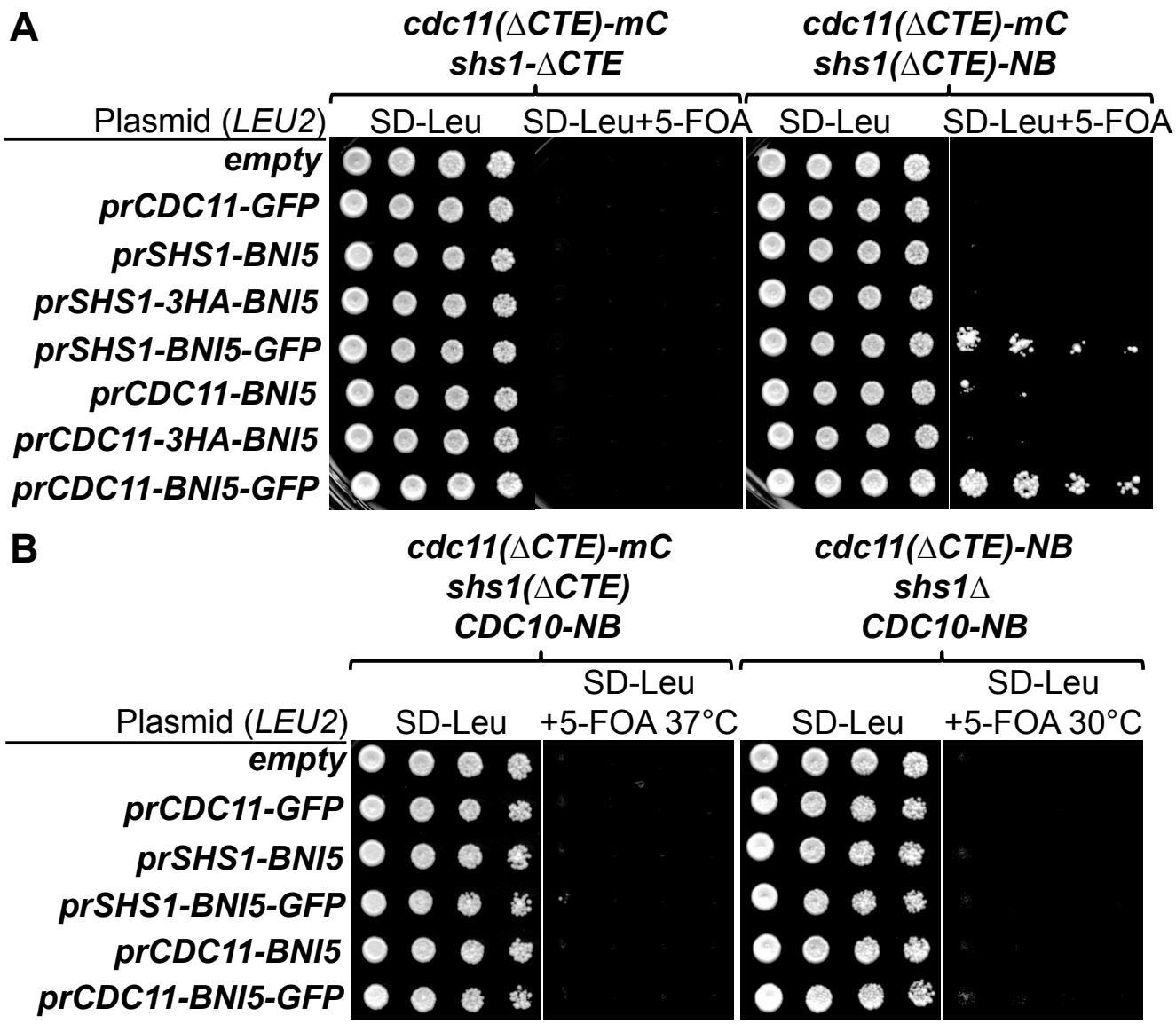

Figure S5. Anti-GFP nanobody-dependent rescue requires that Bni5 carry a GFP tag and cannot be mediated by Cdc10. (A) Strains GFY-861 and GFY-1295 were transformed with plasmids expressing the indicated expression constructs (pRS315, pGF-IVL216, pGF-IVL384, pGF-IVL385, and pGF-IVL629 through pGF-IVL632), grown overnight in SD-Ura-Leu medium at 30ºC, spotted onto medium with or without 5-FOA to counter-select the covering plasmid, and incubated at 37ºC for 3 days prior to imaging. (B) Strains GFY-1462 and GFY-1463 contained the anti-GFP nanobody fused to the C-terminus of Cdc10 were constructed and transformed with the same vectors used in Part A and assayed as previously described. NB, anti-GFP nanobody.

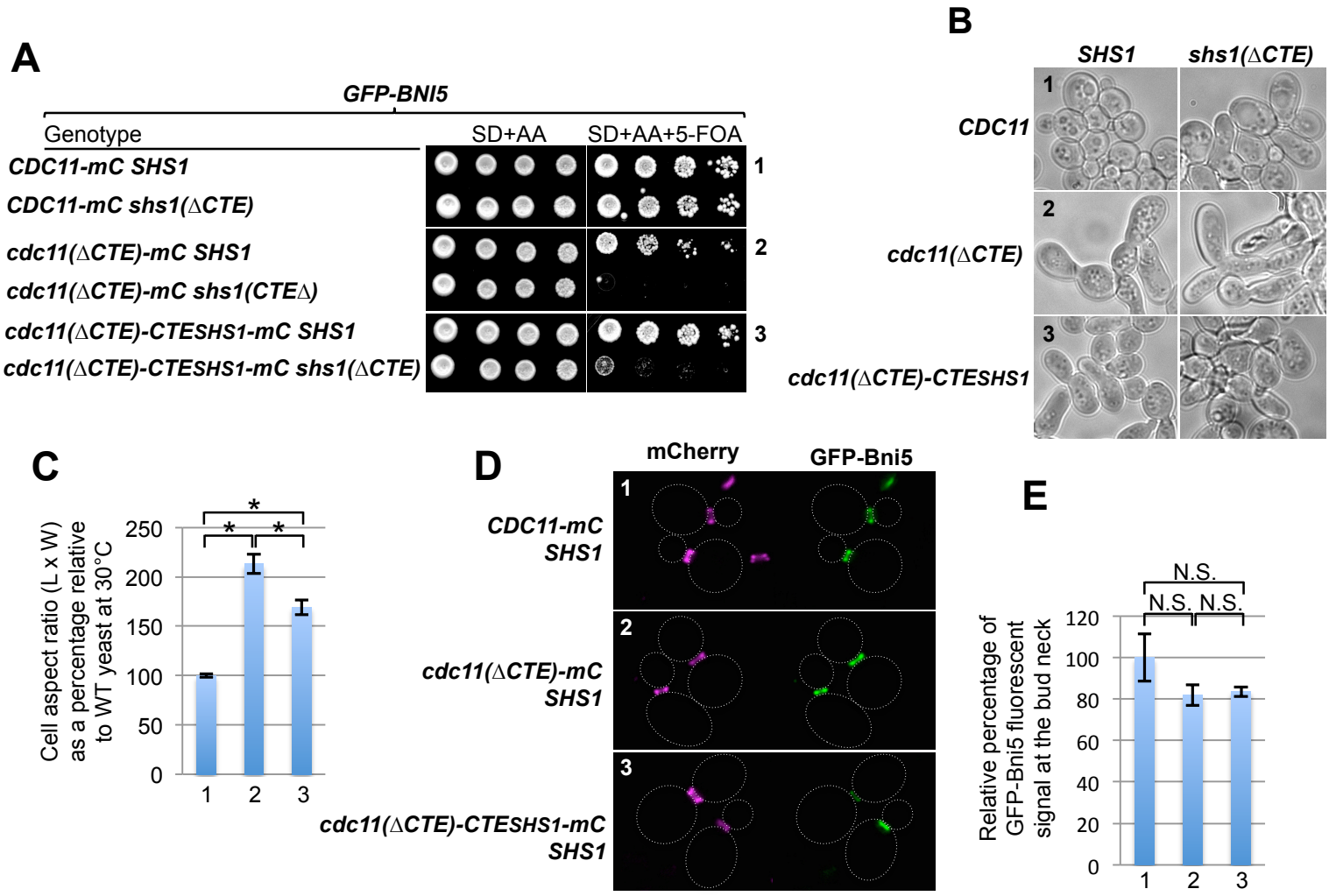

Figure S6. Shs1 CTE is sufficient to retain near-normal morphology and for near-normal recruitment of Bni5 in CTE-less Cdc11 cells. (A) Yeast strains GFY-1324, GFY-1325, GFY-1465, GFY-1466, GFY-1439, and GFY-1440 were grown overnight in SD-Ura at 30°C and spotted onto medium with and without 5-FOA to counterselect the covering *URA3*-marked *CDC11*-expressing plasmid. (B) The three indicated strains (1, 2 and 3; GFY-1324, GFY-1465 and GFY-1439) from (*A*) were selected twice on 5-FOA medium at room temperature to remove the covering plasmid, incubated overnight in YPD at 25°C, and visualized by DIC microscopy. (C) The aspect ratio (length vs. width) of individual cells (n = 50-100) from (*B*) was measured using ImageJ and plotted as a percentage relative to WT. Triplicate cultures of each strain were examined; error is standard deviation of the mean. Asterisk, statistically significant difference ($p < 0.05$, as judged by an unpaired t-test). (D) The same strains from (*B*) were visualized by fluorescence microscopy. (E) The fluorescence intensity of the bud neck (GFP-Bni5) signal for representative cells (n = 50-125) in triplicate cultures of the same strains shown in (*B*) was quantified for those cells that showed a clear-cut septin collar (mCherry signal) using ImageJ after subtraction of background fluorescence, and normalized to the control cells (strain 1), which was set at 100% (error is standard deviation of the mean). N.S., no statistically significant difference ($p > 0.05$, using an unpaired t-test).

Table S1. Yeast strains used to obtain the data shown in Figures S1 to S5 and Table S3.

Strain	Genotype	Reference
GFY-160	BY4741; *cdc11Δ::CDC11::mCherry::SpHIS5^R shs1Δ::SHS1::eGFP::Nat^R + pJT1520*	(FINNIGAN *et al.* 2015)
GFY-162	BY4741; *cdc11Δ::cdc11(Δ357-415)::mCherry::SpHIS5 shs1Δ::shs1(Δ349-551)::eGFP::Nat^R + pJT1520*	(FINNIGAN *et al.* 2015)
GFY-911	BY4741; *cdc11Δ::cdc11(Δ357-415)::mCherry::SpHIS5 shs1Δ::SHS1::BNI5::eGFP::Nat^R + pJT1520*	This study
GFY-1104	BY4741; *cdc11Δ::cdc11(Δ357-415)::mCherry::SpHIS5 shs1Δ::SHS1::BNI5::eGFP::Nat^R bni5Δ::Kan^R + pJT1520*	This study
GFY-913	BY4741; *cdc11Δ::cdc11(Δ357-415)::mCherry::SpHIS5 shs1Δ::shs1(Δ349-551)::BNI5::eGFP::Nat^R + pJT1520*	This study
GFY-1105	BY4741; *cdc11Δ::cdc11(Δ357-415)::mCherry::SpHIS5 shs1Δ::shs1(Δ349-551)::BNI5::eGFP::Nat^R bni5Δ::Kan^R + pJT1520*	This study
GFY-888	BY4741; *cdc11Δ::cdc11(Δ357-415)::mCherry::SpHIS5 shs1Δ::SHS1::eGFP::BNI5::Nat^R + pJT1520*	This study
GFY-1102	BY4741; *cdc11Δ::cdc11(Δ357-415)::mCherry::SpHIS5 shs1Δ::SHS1::eGFP::BNI5::Nat^R bni5Δ::Kan^R + pJT1520*	This study
GFY-890	BY4741; *cdc11Δ::cdc11(Δ357-415)::mCherry::SpHIS5 shs1Δ::shs1(Δ349-551)::eGFP::BNI5::Nat^R + pJT1520*	This study
GFY-1103	BY4741; *cdc11Δ::cdc11(Δ357-415)::mCherry::SpHIS5 shs1Δ::shs1(Δ349-551)::eGFP::BNI5::Nat^R bni5Δ::Kan^R + pJT1520*	This study
GFY-861	BY4741; *cdc11Δ::cdc11(Δ357-415)::mCherry::SpHIS5*	This study

	shs1Δ::shs1(Δ349-551)::Nat^R + pJT1520	
GFY-1295	BY4741; *cdc11Δ::cdc11(Δ357-415)::mCherry::SpHIS5 shs1Δ::shs1(Δ349-551)::NanoBody::Nat^R + pJT1520*	This study
GFY-1462	BY4741; *cdc11Δ::cdc11(Δ357-415)::Hyg^R shs1Δ::Nat^R cdc10Δ::CDC10::NanoBody::SpHIS5+ pJT1520*	This study
GFY-1463	BY4741; *cdc11Δ::cdc11(Δ357-415)::mCherry::Hyg^R shs1Δ::shs1(Δ349-551)::Nat^R cdc10Δ::CDC10::NanoBody::SpHIS5 + pJT1520*	This study
GFY-122	BY4741; *cdc11Δ::cdc11(Δ357-415)::mCherry::SpHIS5 + pJT1520*	(FINNIGAN *et al.* 2015)
GFY-166	BY4741; *cdc11Δ::cdc11(Δ357-415)::mCherry::SpHIS5 shs1Δ::Hyg^R + pJT1520*	(FINNIGAN *et al.* 2015)
GFY-847	BY4741; *cdc11Δ::cdc11(Δ357-415)::mCherry::SpHIS5 bni5Δ::Kan^R + pJT1520*	This study
GFY-1167	BY4741; *cdc11Δ::cdc11(Δ357-415)::mCherry::SpHIS5 bni5Δ::HA$_3$::BNI5::Nat^R + pJT1520*	This study
GFY-1168	BY4741; *cdc11Δ::cdc11(Δ357-415)::mCherry::SpHIS5 bni5Δ::HA$_3$::BNI5::GFP::Nat^R + pJT1520*	This study
GFY-1236	BY4741; *cdc11Δ::cdc11(Δ357-415)::mCherry::SpHIS5 bni5Δ::BNI5::GFP::Nat^R + pJT1520*	This study
GFY-1237	BY4741; *cdc11Δ::cdc11(Δ357-415)::mCherry::SpHIS5 bni5Δ::GFP$_3$::BNI5::Nat^R + pJT1520*	This study
GFY-1238	BY4741; *cdc11Δ::cdc11(Δ357-415)::mCherry::SpHIS5 bni5Δ::HA$_3$::GFP::BNI5::Nat^R + pJT1520*	This study
GFY-1319	BY4741; *CDC10::mCherry^g::Kan^R*	This study

	bni5Δ::GFP::BNI5::SpHIS5 cdc11Δ::CDC11::Hyg^R shs1Δ::Nat^R + pJT1520	
GFY-870	BY4741; *cdc11Δ::cdc11(Δ357-415)::Hyg^R shs1Δ::shs1(Δ349-551)::Nat^R + pJT1520*	This study
GFY-1113	BY4741; *cdc11Δ::cdc11(Δ357-415)::Hyg^R shs1Δ::shs1(Δ349-551)::Nat^R bni5Δ::Kan^R + pJT1520*	This study
BY4741	*MAT**a** leu2Δ ura3Δ met15Δ his3Δ*	(BRACHMANN *et al.* 1998)
GFY-169	BY4741; *cdc11Δ::cdc11(Δ357-415)::Hyg^R shs1Δ::shs1(Δ349-551)::GFP::Nat^R + pJT1520*	This study
GFY-726	BY4741; *cdc11Δ::cdc11(Δ357-415)::Hyg^R shs1Δ::Kan^R + pJT1520*	(FINNIGAN *et al.* 2015)
GFY-1468	BY4741; *cdc11Δ::cdc11(Δ357-415)::Hyg^R shs1Δ::shs1(Δ349-551)::Nat^R bni5Δ::GFP::BNI5::SpHIS5 + pJT1520*	This study
GFY-1324	BY4741; *cdc11Δ::cdc11(1-308)::shs1(349-551)::mCherry::Hyg^R shs1Δ::SHS1::Nat^R bni5Δ::GFP::BNI5::SpHIS5 + pJT1520*	This study
GFY-1325	BY4741; *cdc11Δ::cdc11(1-308)::shs1(349-551)::mCherry::Hyg^R shs1Δ::shs1(349-551Δ)::Nat^R bni5Δ::GFP::BNI5::SpHIS5 + pJT1520*	This study
GFY-1465	BY4741; *cdc11Δ::cdc11(Δ357-415)::mCherry::Hyg^R shs1Δ::SHS1::Nat^R bni5Δ::GFP::BNI5::SpHIS5 + pJT1520*	This study
GFY-1466	BY4741; *cdc11Δ::cdc11(Δ357-415)::mCherry::Hyg^R shs1Δ::shs1(Δ349-551)::Nat^R bni5Δ::GFP::BNI5::SpHIS5*	This study

	+ pJT1520	
GFY-1439	BY4741; *cdc11Δ::CDC11::mCherry::Hyg^R SHS1 bni5Δ::GFP::BNI5::SpHIS5 + pJT1520*	This study
GFY-1440	BY4741; *cdc11Δ::CDC11::mCherry::Hyg^R shs1Δ::shs1(Δ349-551)::Nat^R bni5Δ::GFP::BNI5::SpHIS5 + pJT1520*	This study

Table S2. Plasmids used used to obtain the data shown in Figures S1 to S5 and Table S3.

Plasmid	Description	Reference
pRS315	*CEN, LEU2*	(SIKORSKI AND HIETER 1989)
pGF-IVL216	pRS315 *prCDC11::GFP::Kan^R*	This study
pGF-IVL384	pRS315 *prSHS1::BNI5::eGFP::Nat^R*	This study
pGF-IVL385	pRS315 *prCDC11::BNI5::eGFP::Nat^R*	This study
pGF-IVL629	pRS315 *prSHS1::HA$_3$::BNI5::Kan^R*	This study
pGF-IVL630	pRS315 *prSHS1::BNI5::Kan^R*	This study
pGF-IVL631	pRS315 *prCDC11::HA^3::BNI5::Kan^R*	This study
pGF-IVL632	pRS315 *prCDC11::BNI5::Kan^R*	This study
pGF-IVL341	pRS315 *prGAL1/10::CDC5::eGFP::SpHIS5*	This study
pGF-IVL303	pRS315 *prGAL1/10::IQG1::eGFP::SpHIS5*	This study
pGF-IVL355	pRS315 *prGAL1/10::BUD3::eGFP::SpHIS5*	This study
pGF-IVL329	pRS315 *prGAL1/10::GIC2::eGFP::SpHIS5*	This study
pGF-IVL346	pRS315 *prGAL1/10::RGA1::eGFP::SpHIS5*	This study
pGF-IVL339	pRS315 *prGAL1/10::BUD4::eGFP::SpHIS5*	This study
pGF-IVL348	pRS315 *prGAL1/10::SKT5::eGFP::SpHIS5*	This study
pGF-IVL349	pRS315 *prGAL1/10::SVL3::eGFP::SpHIS5*	This study
pGF-IVL331	pRS315 *prGAL1/10::NIS1::eGFP::SpHIS5*	This study
pGF-IVL347	pRS315 *prGAL1/10::RGD1::eGFP::SpHIS5*	This study
pGF-IVL345	pRS315 *prGAL1/10::HOF1::eGFP::SpHIS5*	This study
pGF-IVL333	pRS315 *prGAL1/10::MLC2::eGFP::SpHIS5*	This study
pGF-IVL332	pRS315 *prGAL1/10::BIL1::eGFP::SpHIS5*	This study
pGF-IVL305	pRS315 *prGAL1/10::KCC4::eGFP::SpHIS5*	This study

pGF-IVL358	pRS315 *prGAL1/10::BNI4::eGFP::SpHIS5*	This study
pGF-IVL343	pRS315 *prGAL1/10::DBF2::eGFP::SpHIS5*	This study
pGF-IVL304	pRS315 *prGAL1/10::GIN4::eGFP::SpHIS5*	This study
pGF-IVL327	pRS315 *prGAL1/10::CHS7::eGFP::SpHIS5*	This study
pGF-IVL334	pRS315 *prGAL1/10::AXL2::eGFP::SpHIS5*	This study
pGF-IVL351	pRS315 *prGAL1/10::BNR1::eGFP::SpHIS5*	This study
pGF-IVL336	pRS315 *prGAL1/10::BEM2::eGFP::SpHIS5*	This study
pGF-IVL337	pRS315 *prGAL1/10::BNI1::eGFP::SpHIS5*	This study
pGF-IVL344	pRS315 *prGAL1/10::ELM1::eGFP::SpHIS5*	This study
pGF-IVL352	pRS315 *prGAL1/10::MYO1::eGFP::SpHIS5*	This study
pGF-IVL330	pRS315 *prGAL1/10::NBA1::eGFP::SpHIS5*	This study
pGF-IVL340	pRS315 *prGAL1/10::BUD6::eGFP::SpHIS5*	This study
pGF-IVL357	pRS315 *prGAL1/10::CLA4::eGFP::SpHIS5*	This study
pGF-IVL302	pRS315 *prGAL1/10::HSL1::eGFP::SpHIS5*	This study
pJT1520/pSB1	pRS316 *URA3 CDC11*	(VERSELE AND THORNER 2004)

Table S3. Summary of overexpression suppression screen.[a]

Yeast Strain	Plasmid	SGlc-Leu 30˚C	SGal-Leu 30˚C	SGal-Leu 37˚C
WT *CDC11 SHS1*	empty vector	+++++	+++++	+++++
WT *CDC11 SHS1*	*CDC5-eGFP*	+++++	+	+
WT *CDC11 SHS1*	*IQG1-eGFP*	+++++	++	++++
WT *CDC11 SHS1*	*BUD3-eGFP*	+++++	+	+
WT *CDC11 SHS1*	*GIC2-eGFP*	+++++	++++	+++
WT *CDC11 SHS1*	*RGA1-eGFP*	+++++	++	++++
WT *CDC11 SHS1*	*BUD4-eGFP*	+++++	+++++	+++++
WT *CDC11 SHS1*	*SKT5-eGFP*	+++++	+++++	+++++
WT *CDC11 SHS1*	*SVL3-eGFP*	+++++	+++++	+++++
WT *CDC11 SHS1*	*NIS1-eGFP*	+++++	+++++	+++++
WT *CDC11 SHS1*	*RGD1-eGFP*	+++++	+++++	+++++
WT *CDC11 SHS1*	*HOF1-eGFP*	+++++	+	++
WT *CDC11 SHS1*	*MLC2-eGFP*	+++++	+++++	+++++
WT *CDC11 SHS1*	*BIL1-eGFP*	+++++	+++++	+++++
WT *CDC11 SHS1*	*KCC4-eGFP*	+++++	+++++	+++++
WT *CDC11 SHS1*	*BNI4-eGFP*	+++++	+	+
WT *CDC11 SHS1*	*DBF2-eGFP*	+++++	++++	+++++
WT *CDC11 SHS1*	*GIN4-eGFP*	+++++	+++	++
WT *CDC11 SHS1*	*CHS7-eGFP*	+++++	+++++	+++++
WT *CDC11 SHS1*	*AXL2-eGFP*	+++++	+++	++
WT *CDC11 SHS1*	*BNR1-eGFP*	+++++	++	++
WT *CDC11 SHS1*	*BEM2-eGFP*	+++++	+++	+++
WT *CDC11 SHS1*	*BNI1-eGFP*	+++++	+	+

WT *CDC11 SHS1*	*ELM1-eGFP*	+++++	+++++	+++++
WT *CDC11 SHS1*	*MYO1-eGFP*	+++++	+	+
WT *CDC11 SHS1*	*NBA1-eGFP*	+++++	+++++	+++++
WT *CDC11 SHS1*	*BUD6-eGFP*	+++++	+++++	+++++
WT *CDC11 SHS1*	*CLA4-eGFP*	+++++	+	+
WT *CDC11 SHS1*	*BNI5-eGFP*	+++++	+++++	+++++
WT *CDC11 SHS1*	*HSL1-eGFP*	+++++	++	+
cdc11-ΔCTE shs1-ΔCTE-GFP	empty vector	+++++	+++++	++
cdc11-ΔCTE shs1-ΔCTE-GFP	*CDC5-eGFP*	+++++	-	-
cdc11-ΔCTE shs1-ΔCTE-GFP	*IQG1-eGFP*	+++++	+++	-
cdc11-ΔCTE shs1-ΔCTE-GFP	*BUD3-eGFP*	+++++	++	-
cdc11-ΔCTE shs1-ΔCTE-GFP	*GIC2-eGFP*	+++++	+	-
cdc11-ΔCTE shs1-ΔCTE-GFP	*RGA1-eGFP*	+++++	+	+
cdc11-ΔCTE shs1-ΔCTE-GFP	*BUD4-eGFP*	+++++	+++++	+++
cdc11-ΔCTE shs1-ΔCTE-GFP	*SKT5-eGFP*	+++++	+++++	++
cdc11-ΔCTE shs1-ΔCTE-GFP	*SVL3-eGFP*	+++++	++	+
cdc11-ΔCTE shs1-ΔCTE-GFP	*NIS1-eGFP*	+++++	+++++	++
cdc11-ΔCTE shs1-ΔCTE-GFP	*RGD1-eGFP*	+++++	++++	-
cdc11-ΔCTE shs1-ΔCTE-GFP	*HOF1-eGFP*	+++++	+	+
cdc11-ΔCTE shs1-ΔCTE-GFP	*MLC2-eGFP*	+++++	+++++	++
cdc11-ΔCTE shs1-ΔCTE-GFP	*BIL1-eGFP*	+++++	+++++	++
cdc11-ΔCTE shs1-ΔCTE-GFP	*KCC4-eGFP*	+++++	+++++	++
cdc11-ΔCTE shs1-ΔCTE-GFP	*BNI4-eGFP*	+++++	-	-
cdc11-ΔCTE shs1-ΔCTE-GFP	*DBF2-eGFP*	+++++	+++	-
cdc11-ΔCTE shs1-ΔCTE-GFP	*GIN4-eGFP*	+++++	++	+

cdc11-ΔCTE shs1-ΔCTE-GFP	*CHS7-eGFP*	+++++	+++++	++
cdc11-ΔCTE shs1-ΔCTE-GFP	*AXL2-eGFP*	+++++	-	-
cdc11-ΔCTE shs1-ΔCTE-GFP	*BNR1-eGFP*	+++++	-	-
cdc11-ΔCTE shs1-ΔCTE-GFP	*BEM2-eGFP*	+++++	-	-
cdc11-ΔCTE shs1-ΔCTE-GFP	*BNI1-eGFP*	+++++	N.T.	N.T.
cdc11-ΔCTE shs1-ΔCTE-GFP	*ELM1-eGFP*	+++++	++++	-
cdc11-ΔCTE shs1-ΔCTE-GFP	*MYO1-eGFP*	+++++	-	-
cdc11-ΔCTE shs1-ΔCTE-GFP	*NBA1-eGFP*	+++++	++++	-
cdc11-ΔCTE shs1-ΔCTE-GFP	*BUD6-eGFP*	+++++	+++++	-
cdc11-ΔCTE shs1-ΔCTE-GFP	*CLA4-eGFP*	+++++	N.T.	N.T.
cdc11-ΔCTE shs1-ΔCTE-GFP	*BNI5-eGFP*	+++++	+++++	+++++
cdc11-ΔCTE shs1-ΔCTE-GFP	*HSL1-eGFP*	+++++	++	+
cdc11-ΔCTE shs1Δ	empty vector	+++++	++++	++
cdc11-ΔCTE shs1Δ	*CDC5-eGFP*	+++++	-	-
cdc11-ΔCTE shs1Δ	*IQG1-eGFP*	+++++	N.T.	N.T.
cdc11-ΔCTE shs1Δ	*BUD3-eGFP*	+++++	-	-
cdc11-ΔCTE shs1Δ	*GIC2-eGFP*	+++++	-	-
cdc11-ΔCTE shs1Δ	*RGA1-eGFP*	+++++	-	-
cdc11-ΔCTE shs1Δ	*BUD4-eGFP*	+++++	-	-
cdc11-ΔCTE shs1Δ	*SKT5-eGFP*	+++++	+++	+
cdc11-ΔCTE shs1Δ	*SVL3-eGFP*	+++++	+	-
cdc11-ΔCTE shs1Δ	*NIS1-eGFP*	+++++	+++	+++
cdc11-ΔCTE shs1Δ	*RGD1-eGFP*	+++++	-	-
cdc11-ΔCTE shs1Δ	*HOF1-eGFP*	+++++	-	-
cdc11-ΔCTE shs1Δ	*MLC2-eGFP*	+++++	++++	+

cdc11-ΔCTE shs1Δ	*BIL1-eGFP*	+++++	N.T.	N.T.
cdc11-ΔCTE shs1Δ	*KCC4-eGFP*	+++++	++	+
cdc11-ΔCTE shs1Δ	*BNI4-eGFP*	+++++	-	-
cdc11-ΔCTE shs1Δ	*DBF2-eGFP*	+++++	N.T.	N.T.
cdc11-ΔCTE shs1Δ	*GIN4-eGFP*	+++++	+	+
cdc11-ΔCTE shs1Δ	*CHS7-eGFP*	+++++	++	-
cdc11-ΔCTE shs1Δ	*AXL2-eGFP*	+++++	-	-
cdc11-ΔCTE shs1Δ	*BNR1-eGFP*	+++++	+	-
cdc11-ΔCTE shs1Δ	*BEM2-eGFP*	+++++	N.T.	N.T.
cdc11-ΔCTE shs1Δ	*BNI1-eGFP*	+++++	N.T.	N.T.
cdc11-ΔCTE shs1Δ	*ELM1-eGFP*	+++++	+	+
cdc11-ΔCTE shs1Δ	*MYO1-eGFP*	+++++	-	-
cdc11-ΔCTE shs1Δ	*NBA1-eGFP*	+++++	+	-
cdc11-ΔCTE shs1Δ	*BUD6-eGFP*	+++++	++	-
cdc11-ΔCTE shs1Δ	*CLA4-eGFP*	+++++	-	-
cdc11-ΔCTE shs1Δ	*BNI5-eGFP*	+++++	+++++	++++
cdc11-ΔCTE shs1Δ	*HSL1-eGFP*	+++++	-	-

[a]Strain BY4741 (*CDC11 SHS1*), GFY-169 (*cdc11-ΔCTE shs1-ΔCTE*) or GFY-726 (*cdc11-ΔCTE shs1Δ*), each harboring a URA3-marked vector expressing WT CDC11, was transformed, as indicated, with a *LEU2*-based vector expressing under control of the *GAL1/10* promoter the gene of interest tagged at its C-terminus with eGFP. The resulting transformants were grown to mid-exponential phase, and then streaked twice on -Leu medium containing 5-FOA to select against the covering plasmid (expressing WT *CDC11*). The resulting derivatives were incubated overnight in -Leu Raf-Suc medium at room temperature, and then serial dilutions were spotted onto plates containing either SGlc-Leu or SGal-Leu medium, as indicated, and incubated for two days at either 30ºC or 37ºC. Growth under each condition was assessed by comparison to the parent yeast strain containing empty vector (pRS315): +++++, growth equivalent to the WT control; ++++, growth slightly less robust than the WT control; +++, growth detectably weaker than the WT control; ++, growth significantly slower than WT control; +, very weak growth; -, no detectable growth; N.T., not tested.

SUPPLEMENTAL REFERENCES

Brachmann, C. B., A. Davies, G. J. Cost, E. Caputo, J. Li *et al.*, 1998 Designer deletion strains derived from *Saccharomyces cerevisiae* S288C: a useful set of strains and plasmids for PCR-mediated gene disruption and other applications. Yeast **14:** 115-132.

Finnigan, G. C., J. Tagakii, C. Cho and J. Thorner, 2015 Comprehensive genetic analysis of paralogous terminal septin subunits Shs1 and Cdc11 in *Saccharomyces cerevisiae.* Genetics**,** accompanying manuscript.

Kelley, L. A., and M. J. E. Sternberg, 2009 Protein structure prediction on the Web: a case study using the Phyre server. Nat. Protoc. **4:** 363 - 371.

Neumann, R. S., S. Kumar, T. H. Haverkamp and K. Shalchian-Tabrizi, 2014 BLASTGrabber: a bioinformatic tool for visualization, analysis and sequence selection of massive BLAST data. BMC Bioinformatics **15:** 128.1-128.11.

Sikorski, R. S., and P. Hieter, 1989 A system of shuttle vectors and yeast host strains designed for efficient manipulation of DNA in *Saccharomyces cerevisiae*. Genetics **122:** 19-27.

Thompson, J. D., D. G. Higgins and T. J. Gibson, 1994 CLUSTAL W: improving the sensitivity of progressive multiple sequence alignment through sequence weighting, position-specific gap penalties and weight matrix choice. Nucleic Acids Res. **22:** 4673-4680.

Versele, M., and J. Thorner, 2004 Septin collar formation in budding yeast requires GTP binding and direct phosphorylation by the PAK, Cla4. J. Cell Biol. **164:** 701-715.